



A survey of helium isotopes in Icelandic volcanic materials and geothermal fluids using spatial analyses in ArcGIS

Sunna Harðardóttir



**Faculty of Earth Science
University of Iceland
2016**

A survey of helium isotopes in Icelandic volcanic materials and geothermal fluids using spatial analysis in ArcGIS

Sunna Harðardóttir

10 ECTS thesis submitted in partial fulfilment of
Baccalaureus Scientiarum degree in Geology

Advisor
Sæmundur Ari Halldórsson

Faculty of Earth Science
School of Engineering and Natural Sciences
University of Iceland
Reykjavík, June 2016

A survey of helium isotopes in Icelandic volcanic materials and geothermal fluids using spatial analysis in ArcGIS
A survey of helium isotopes in Iceland
10 ETCS thesis submitted in partial fulfillment of *Baccalaureus Scientiarum* degree in Geology

Copyright © 2016 Sunna Harðardóttir
All rights reserved

Faculty of Earth Science
School of Engineering and Natural Sciences
University of Iceland
Askja, Sturlugata 7
101 Reykjavík

Telephone: 525 4000

Registration information:
Sunna Harðardóttir, 2016, *A survey of helium isotopes in Icelandic volcanic materials and geothermal fluids using spatial analysis in ArcGIS*, BS thesis, Faculty of Earth Science, University of Iceland, pp. 60.

Printing: Háskólaprent
Reykjavík, June 2016

Abstract

The distribution of helium isotope ratios ($^3\text{He}/^4\text{He}$) in Icelandic geothermal fluids, volcanic glasses and phyrlic lavas was investigated. Published data from previous studies were compiled and a data base with all available data constructed. Modifications of primary (i.e., mantle-derived) helium isotope ratios, due to additions of, for example, air-derived helium and radiogenic ingrowth, were evaluated and the data base was filtered accordingly. The geographical information system ArcGIS (ESRI) was used to perform spatial analysis on the filtered data base. An interpolation method called Natural Neighbor was used to calculate representative helium isotope ratios for all parts of Iceland, including off-axis regions. In accordance to prior studies, the results show that helium isotope ratios in the whole of Iceland vary from 5.1 to 37.7 R_A (where R_A is the $^3\text{He}/^4\text{He}$ ratio of air (Füri et al., 2010)). However, this study allows for a fine-scale distinction to be made between individual rift segments and off-rift regions. The results clearly reveal that each rift zone has its own distinctive isotope signature: 12-17 R_A in the Western Rift Zone (WRZ), 8-11 R_A in the Northern Rift Zone (NRZ) and 18-21 R_A in the Eastern Rift Zone (ERZ). A high helium plateau, characterized by values $\geq 20 R_A$ is located in Central Iceland and covers an area of 85×50 km. This plateau continues down the propagating ERZ and through the South Iceland Seismic Zone (SISZ) and coincides with many geological features, e.g., eruption rates, seismic velocity and gravity anomalies. Such high helium isotope ratios have been associated with undegassed and primordial mantle sources that have been isolated in the lower mantle over Earth's history. The high helium plateau therefore, marks the conduit of the mantle plume underlying central Iceland.

Útdráttur

Dreifing helíum samsætna var rannsökuð í íslenskum jarðhitavökvum, glerjum og dílóttum hraunum. Útgefnum gögnum frá fyrri rannsóknum var safnað saman og út frá þeim var settur saman gagnagrunnur. Breytingar á upphaflegu samsætuhlutfalli helíums, vegna til dæmis, helíums sem er upprunið í lofti og myndunnar ^4He við geislavirkt niðurbrot, voru metnar og gagnagrunnurinn var síaður í samræmi við það. Landupplýsingakerfið ArcGIS (ESRI) var notað til að framkvæma rýmdargreiningar á síuðu gagnasafninu. Brúunaraðferðin Natural Neighbor var notuð til að reikna samsætuhlutfall helíums fyrir allt landið, þar með talið svæði utan rek- og gosbelta. Í samræmi við fyrri rannsóknir, sýna niðurstöðurnar að samsætuhlutfall helíums fyrir allt Ísland nær frá 5.1 til 37.7 R_A (þar sem R_A er hlutfall $^3\text{He}/^4\text{He}$ í andrúmslofti (Füri et al., 2010)). Þessi rannsókn gefur hins vegar möguleika á aðgreiningu milli mismunandi rekbelta og svæða utan þeirra. Niðurstöðurnar sýna greinilega að öll gliðnunarbelti landsins hafa sitt einkennandi samsætuhlutfall: 12-17 R_A fyrir vestra gliðnunarbeltið (WRZ), 8-11 R_A fyrir nyrðra gliðnunarbeltið (NRZ) og 18-21 R_A fyrir eystra gliðnunarbeltið (ERZ). Hágilda helíum svæði sem einkennist af gildum $\geq 20 R_A$ er staðsett yfir miðju Íslandi og þekur svæði sem er 85×50 km. Þetta svæði heldur áfram niður eftir eystra gliðnunarbeltinu (ERZ) og í gegnum þverbrotabeltið á Suðurlandi (SISZ) og samsvarar öðrum jarðfræðilegum einkennum, t.d. tíðni eldgosa, hraða jarðskjálftabylgna og þyngdarfrávikum. Þessi háu samsætuhlutföll helíums hafa verið tengd við óafgasaða frummöttulgeyma sem hafa verið einangraðir í neðri möttli frá árdögum jarðar. Þar af leiðandi afmarkar hágilda helíum svæðið rás möttulstróksins undir Íslandi.

Table of contents

Figures	ix
Tables.....	xi
Abbreviation	xii
Acknowledgements	xiii
1 Introduction.....	1
2 Geochemistry of helium and its isotopes.....	3
2.1 Helium and helium isotopes in Earth	3
2.2 Helium in terrestrial reservoirs.....	4
2.2.1 MORB.....	4
2.2.2 OIB.....	5
2.2.3 SCLM.....	5
2.3 Helium studies in Iceland	5
2.3.1 Early studies utilizing geothermal fluids	5
2.3.2 Studies on recent volcanic glasses and phyric lavas.....	5
2.3.3 Helium studies in older parts of the Icelandic crust.....	6
2.3.4 Cosmogenic dating studies utilizing ^3He	6
3 Geological setting	7
4 Methods.....	9
4.1 Evaluation of the data base and filtering criterion	10
4.1.1 Air contamination	10
4.1.2 Helium concentration.....	11
4.1.3 Duplicate samples	12
4.1.4 Samples from the same general region yielding different results.....	13
4.1.5 Other problems.....	13
4.2 Methods in ArcGIS	13
5 Results	15
5.1 Geothermal fluids	15
5.2 Subglacial lavas	16
5.3 Phyric lavas	17
5.4 Combined data.....	18
5.5 Filtered data.....	18
5.6 Interpolation	19
6 Discussion	21
6.1 Regional variability	21
6.1.1 The active rift zones and the SISZ.....	21
6.1.2 Vestfirðir	22

6.1.3	Volcanic flank zones	22
6.2	Consistency between geothermal fluids, volcanic glasses and phyric lavas.....	23
6.3	Comparison with geophysical data	26
6.4	Implications for the Iceland plume structure	28
7	Conclusions	29
	References	31
	Appendix	35

Figures

Figure 1: Helium isotope ratios in different reservoirs	4
Figure 2: The neovolcanic zones of Iceland	8
Figure 3: Helium isotope ratios plotted against the X-factor for geothermal fluids, glasses and phenocrysts	11
Figure 4: Helium isotope ratios plotted against helium concentrations for volcanic glasses	12
Figure 5: Helium isotope ratios plotted against helium concentrations for phenocrysts	12
Figure 6: Helium isotope ratios for geothermal fluids	15
Figure 7: Helium isotope ratios for volcanic glasses	16
Figure 8: Helium isotope ratios for phenocrysts	17
Figure 9: Helium isotope ratios for the combined data	18
Figure 10: Helium isotope ratios for the filtered data	19
Figure 11: Representative helium isotope ratios calculated with the Natural Neighbor method, areas where no sampling has occurred are shown with the dashed line	20
Figure 12: Contours that connect the same helium isotope ratios	20
Figure 13: Histograms showing the helium isotope ratios along different rift zones and the SISZ	21
Figure 14: Helium isotope ratios in different sample phases along the western NRZ plotted against latitude	23
Figure 15: Helium isotope ratios in different sample phases along the eastern NRZ plotted against latitude	24
Figure 16: Helium isotope ratios in different sample phases along the WRZ and geothermal fluids from the SISZ plotted against longitude	25
Figure 17: Helium isotope ratios in different sample phases along the ERZ and the SIVZ and geothermal fluids from the SISZ plotted against latitude	25
Figure 18: Helium isotope ratios in different sample phases along the SNVZ plotted against longitude	26

Figure 19: The Bouguer gravity anomaly over Iceland	27
--	-----------

Tables

<i>Table 1: Articles used to construct the data base</i>	9
--	---

Abbreviation

MORB - Mid Ocean Ridge Basalt

OIB - Ocean Island Basalt

SCLM - Sub-Continental Lithospheric Mantle

WRZ - Western Rift Zone

ERZ - Eastern Rift Zone

SISZ - South Iceland Seismic Zone

NRZ - Northern Rift Zone

SIVZ - South Iceland Volcanic Zone

TFZ - Tjörnes Fracture Zone

ÖVZ - Öräfajökull Volcanic Zone

SNVZ - Snæfellsnes Volcanic Zone

Ma - Million years

km - Kilometers

cm - Centimeters

N - North

E - East

W - West

STP - Standard temperature and pressure

ncm³ - Cubic Nano centimeters

g - Grams

mGal - Milli Gal

Acknowledgements

I wish to thank my advisor Sæmundur Ari Halldórsson for proposing this project and for professional guidance. Gunnlaugur Magnús Einarsson is thanked for his help with analysis in ArcGIS. Finally I would like to thank my sister Daney Harðardóttir for reviewing this thesis.

1 Introduction

Helium is a noble gas that is chemically inert. It has two naturally occurring isotopes, ^3He and ^4He , that have contrasting origins (Graham, 2002). Helium isotopes are valuable tracers in a number of geological processes, especially in processes related to mantle geochemistry. Mantle-derived materials are enriched in ^3He relative to ^4He , over three orders of magnitude, compared to He produced by radioactive decay in the continents (Hilton et al., 1990).

Iceland is located at a divergent plate boundary and is also a hotspot (Einarsson, 2008). The result of this unique geological setting is a broad range in the helium isotope ratio, where both mid ocean ridge basalt (MORB) and ocean island basalt (OIB) ratios are observed. The distribution of the helium isotopes can be used to get a better understanding of the mantle plume beneath Iceland. The observations of ^3He enrichments in the mantle have been used to make inferences about its deep structure and evolutionary history (Hilton et al., 1990).

In this study the helium isotope ratio (R/R_A) in geothermal fluids, volcanic glasses and phyric lavas from Iceland was investigated. The objective of this study is to compile previously published data about helium isotopes reported from Iceland. A data base, with a total of 707 samples, was constructed from published data. The data was filtered, since air-derived helium can contaminate the samples. The filtered data base was used to conduct spatial analysis in ArcGIS and investigate the regional variability of the helium isotope ratio in Iceland. The results of these analysis are compiled and displayed on maps. This study demonstrates that the $^3\text{He}/^4\text{He}$ ratio correlates with geophysical measurements, e.g. seismic velocity and gravity parameters which have implications for depicting the structuring of the Iceland mantle plume.

2 Geochemistry of helium and its isotopes

2.1 Helium and helium isotopes in Earth

Helium is a noble gas, which has a filled outer electron shell. This makes helium chemically inert and volatile. Helium is the second lightest element and the second most abundant element in the universe, with an abundance of 25%. As with other light elements, helium formed during the Big Bang and is being created by nuclear fusion of hydrogen in stars (White, 2013). The first evidence of helium was observed during the solar eclipse in 1868 as an unknown yellow line in the spectrum of sunlight. Twenty seven years later, in 1895 William Ramsay isolated helium on Earth by extracting it from a uranium mineral (Petrucchi et al., 2011).

Two naturally occurring isotopes of helium exist, ^3He and ^4He . Helium-4 is much more abundant relative to ^3He , as it is constantly forming in Earth's materials by radioactive decay. Alpha-particles (α) are ^4He nuclei, so ^4He is produced by α -decay of ^{238}U , ^{235}U , ^{232}Th and other decay series elements over geological time. On the other hand nearly all of ^3He is primordial. Degassing from the Earth's interior is the most important terrestrial source of ^3He . Other sources of ^3He to the atmosphere are the auroral precipitation of solar wind, direct accretion from cosmic rays and flux of cosmic dust and meteorites. Small but measureable quantities of ^3He are produced in rocks at the Earth's surface by high energy cosmic rays, mostly from spallation of O, Si, Mg and Fe atoms. Very small quantities of ^3He are produced by the nuclear reaction $^6\text{Li}(n,\alpha)\rightarrow^3\text{H}(\beta)\rightarrow^3\text{He}$, which is a part of the radioactive decay of U and Th. In this reaction ^6Li is excited by a capture of a neutron, It decays through the emission of an alpha particle to tritium. The tritium then beta decays to ^3He (Graham, 2002).

Helium is not preserved on Earth, therefore much of the helium present when the Earth formed, has been lost. It diffuses very rapidly and therefore any helium brought to Earth's surface finds its way quickly into the atmosphere. When it reaches the top of the atmosphere it will eventually escape from Earth's gravity because of its low mass. (White, 2013). This gravitational escape from the thermosphere and helium's short atmospheric residence time of 1 to 10 Ma causes it not to be recycled by plate tectonics to the Earth's interior. This makes the $^3\text{He}/^4\text{He}$ ratio unique among isotope tracers of mantle sources (Graham, 2002).

The isotope ratio of $^4\text{He}/^3\text{He}$ varies in the Earth. ^4He is continually produced, through radioactive decay, but ^3He is not so the $^4\text{He}/^3\text{He}$ ratio in the Earth is a very large number. The isotope ratio of helium is generally expressed as $^3\text{He}/^4\text{He}$, (R). This is in contradiction to the regular convention of placing the radiogenic isotope in the numerator. The atmospheric ratio of $^3\text{He}/^4\text{He}$ (R_A), is uniform and therefore makes a convenient standard and provides the basis for a convenient normalization. The $^3\text{He}/^4\text{He}$ ratio of the atmosphere (R_A), is 1.384×10^{-6} and helium isotope ratios are reported and discussed relative to the atmospheric value (R/R_A) (White, 2013). The absolute terrestrial $^3\text{He}/^4\text{He}$ ratio varies by

several orders of magnitude from high values ($>10^{-5}$) in mantle-derived lavas and fluids, to low values ($\sim 10^{-8}$) in continental regions due to increased amounts of radiogenic ^4He (Graham, 2002).

The most reliable noble gas samples are subglacial and oceanic lavas. These lavas cool rapidly and form quenched rims of glass that trap measureable amounts of volatiles, including helium. Subaerial basalts are of little use in analysis of noble gases since they are largely degassed. However minerals like olivine and pyroxene can trap noble gases in melt or fluid inclusions during crystal growth (Kurz et al. 1982; Graham 2002).

2.2 Helium in terrestrial reservoirs

Helium isotope ratio differs in various reservoirs (Figure 1). Figure 1 shows both the absolute terrestrial $^3\text{He}/^4\text{He}$ ratio and the normalized ratio (R/R_A) in various terrestrial and solar system materials. The highest $^3\text{He}/^4\text{He}$ ratios are cosmogenic and higher ratios are measured in meteorites and at the Sun than on the Earth. The highest ratios on Earth are measured in OIBs, while the lowest ratios are observed in crustal rocks. In Iceland two reservoirs exist, MORB and OIB, which show different values and ranges for the $^3\text{He}/^4\text{He}$ ratio. Below, the helium isotope ratios of MORB, OIB and sub-continental lithospheric mantle (SCLM) will be discussed in more detail, since these three reservoirs form magmas.

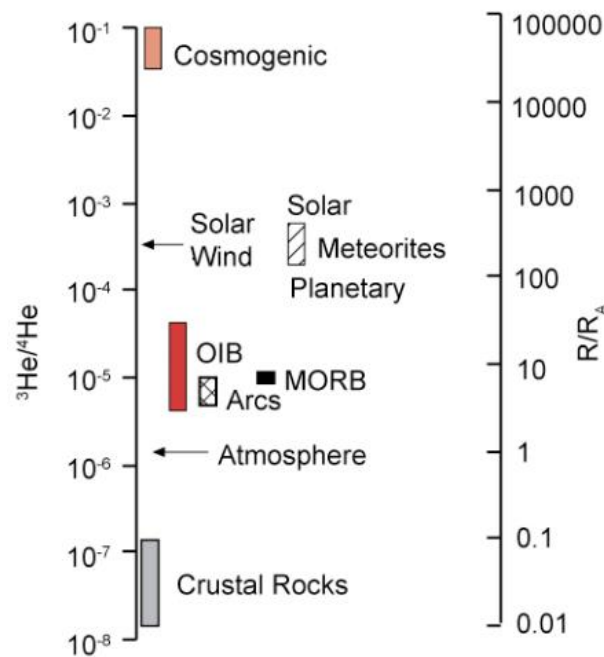


Figure 1: Helium isotope ratios in different reservoirs (White, 2013)

2.2.1 MORB

MORBs are basalts that erupt at mid-ocean ridges where new oceanic crust is continually forming as tectonic plates diverge. MORB is olivine and quartz-normative tholeiite. (Frost & Frost, 2014). Tholeiitic basalts form by partial melting as the ascending mantle beneath mid-ocean ridges reaches its solidus temperature. MORBs are thought to represent a sampling of the upper mantle that has been argued to be relatively degassed. MORBs have consistent values of $8 \pm 1 R_A$ for the $^3\text{He}/^4\text{He}$ ratio (Graham, 2002).

2.2.2 OIB

OIBs are basalts that erupt at off-ridge, intraplate locations, ocean islands and oceanic plateaus, and includes both tholeiitic and alkali basalts (Frost & Frost, 2014). OIBs have a wider range than MORBs and show high magmatic $^3\text{He}/^4\text{He}$ ratios, values higher than 30 R_A have been reported in locations such as Hawaii and Iceland. The difference observed between MORBs and OIBs in helium isotope ratios is accepted by most investigators as evidence for two distinct mantle source regions (Graham, 2002). The high $^3\text{He}/^4\text{He}$ ratios at OIB localities are usually associated with mantle upwellings or mantle plumes of relatively undegassed mantle that has remained isolated at depth (Breddam et al., 2000). Over geological time these deep regions might have been more or less isolated, resulting in deep regions that are less degassed and have lower time-integrated $(\text{U}+\text{Th})/^3\text{He}$ than shallower mantle sources (Graham, 2002).

2.2.3 SCLM

The mantle portion of continental plates is called the SCLM. It is rather different from the lithosphere beneath the ocean basins and instead of being subducted and recycled, like oceanic lithosphere, the SCLM has largely remained stationary under the overlying continent since its formation (Winter, 2014). The SCLM's mineralogy and geochemistry is different from the oceanic mantle. The SCLM has developed its own signature in terms of major and trace elements and isotope signature, that is distinct from the MORB source. The SCLM has similarities with the depleted oceanic mantle but is re-enriched by fluids either from the asthenosphere or from slab dehydration added during past subductions. Typical SCLM values for the $^3\text{He}/^4\text{He}$ ratio are $6.1 \pm 0.9 R_A$ (Gautheron & Moreira, 2002).

2.3 Helium studies in Iceland

2.3.1 Early studies utilizing geothermal fluids

Russian scientist were the first to analyze helium isotopes in geothermal fluids from Iceland. Polak et al. (1976) made measurements in Iceland to compare with measurements from geothermal fluids and gases from tectonically stable, intraplate, areas. Torgersen and Jenkins (1982) also included measurements of helium isotopes in Icelandic geothermal fluids in their survey of fluids from different geological environments. Results showed that there is a great variety in the isotope composition of helium in different geological environments and Iceland was identified as a region with a high $^3\text{He}/^4\text{He}$ ratio. Hilton et al. (1990) confirmed that excess ^3He is measured in Iceland, both within the neovolcanic zones but also in older parts of the Icelandic crust. The high $^3\text{He}/^4\text{He}$ ratios in the older crust were thought to result from release of magmatic volatiles due to mantle melting rather than dispersion by groundwater flow from the neovolcanic zones (see also section 6.1.2.).

2.3.2 Studies on recent volcanic glasses and phyric lavas

Condomines et al. (1983) were the first to analyze helium isotopes in volcanic glasses. Their results showed a consistent range for basaltic glasses with the previously recorded range for Icelandic geothermal systems. Intermediate and acid samples were all severely contaminated by atmospheric helium and showed values close to 1 R_A . From measured helium isotope ratios in glasses, Kurz et al. (1985) showed, that each rift zone has a

distinctive basaltic $^3\text{He}/^4\text{He}$ isotopic signature. Since then, the highest ratios within the neovolcanic zones (up to $\sim 34 R_A$) have been measured in central Iceland (Breddam et al., 2000; Macpherson et al., 2005). These high values coincide with geophysical measurements and have been connected to the mantle plume situated below Iceland.

Helium and other noble gases have been studied extensively in Icelandic subglacial volcanic glasses in most cases to get a better understanding of mantle sources. Studies of Icelandic subglacial basalts (Harrison et al., 1999; Dixon et al., 2000; Trieloff et al., 2000; Moreira et al., 2001; Dixon, 2003; Füri et al., 2010) have led to the interpretation that high $^3\text{He}/^4\text{He}$ ratios are caused by an undegassed, deep mantle source for mantle plumes. The upper mantle or the MORB source is on the other hand degassed and contains less ^3He (Moreira et al., 2001). In particular have combined studies of He-Ne-Ar-Xe provided crucial evidence supporting a notion that the Icelandic mantle plume source is sampling a primitive and volatile-rich reservoir from early in Earth's history (Mukhopadhyay, 2012).

Helium is still being investigated in Iceland and the latest analysis were conducted by Halldórsson et al. (2016) in which analysis of nitrogen and other noble gases were combined, to investigate the recycling of crustal material by the Icelandic mantle plume.

2.3.3 Helium studies in older parts of the Icelandic crust

In some parts of the older Icelandic crust unusually high $^3\text{He}/^4\text{He}$ ratios have been measured. Polak et al. (1976) measured a value of 23.8 R_A in a geothermal fluid from Hveravík, Vestfirðir. A large number of measurements have been done on both geothermal fluids and phenocrysts from Vestfirðir since then (Hilton et al. 1990; Poreda et al. 1992; Hilton et al., 1998; Hilton et al., 1999; Ellam & Stuart, 2004; Füri et al., 2010). The highest ratio of 37.7 R_A was measured by Hilton et al. (1999) in a phenocryst sample from Selárdalur. In other parts of the older Icelandic crust measurements have not been carried out with the same intensity. The few measurements that have been done in Eastern Iceland show a range of 5.1-14.6 R_A (Kononov & Polak; Poreda et al., 1992; Ellam & Stuart, 2004), which is considerably lower than the range of 6.2-37.7 R_A reported from Vestfirðir.

2.3.4 Cosmogenic dating studies utilizing ^3He

Measurements of ^3He have also been used to determine the age of lavas (Licciardi et al., 2006) and table mountains (Licciardi et al., 2007; Eason et al., 2015) in Iceland. In these studies cosmogenic ^3He production rates in olivine phenocrysts were calculated from the measured $^3\text{He}/^4\text{He}$ ratio. The age of the landforms were then calculated from the ^3He production rate. The results of Licciardi et al. (2006) were similar to previous results gained by using radiocarbon to determine the age of the lavas. No comparison is available for the table mountains, since Licciardi et al. (2007) and Eason et al. (2015) provided the first direct chronology for these landforms.

3 Geological setting

Iceland is a subaerial section of the Mid-Atlantic Ridge, that is distinguished by high basaltic melt production and an anomalously thick crust. (Darbyshire et al., 2000) Iceland is situated at a divergent plate boundary which separates the Eurasia Plate from the North American Plate. The two plates move apart about 2 cm per year in E-W direction. Iceland is a hotspot and is presumed to be fed by a deep mantle plume. The center of the plume is assumed to be located under central Iceland (Einarsson, 2008; Bjarnason, 2008).

The neovolcanic zones are a surface expression of the mid-ocean ridge in Iceland or the zones of active volcanism (Figure 2). The neovolcanic zones are covered with rocks that are younger than 0.8 Ma (Guðmundsson, 2000). There are two types of neovolcanic zones, axial rift zones, that represent the landward extensions of the Mid-Atlantic Ridge, and off-rift volcanic zones. The axial rift zones cross Iceland from southwest to northeast, linking the Reykjanes Ridge in the southwest to the Kolbeinsey Ridge in the north (Figure 2). In the north the Tjörnes Fracture Zone (TFZ) connects Kolbeinsey Ridge to the NRZ, which continues south to Vatnajökull. There the axial rift zone splits up into two branches, the WRZ and the ERZ. The WRZ and the ERZ are separated by the transform fault system, SISZ. The off-rift zones are South Iceland Volcanic Zone (SIVZ), Snæfellsnes Volcanic Zone (SNVZ) and Örfajökull Volcanic Zone (ÖVZ). SIVZ is a direct continuation of the ERZ, but SNVZ and ÖVZ are intraplate and not connected to the active plate boundary. The axial rift zones erupt lava of tholeiitic composition. The off-rift volcanic zones erupt lavas of transitional-alkalic to alkalic composition (Jakobsson et al., 2008).

The Icelandic crust is often considered in terms of three major units (Figure 2). These units are: the Tertiary flood basalts, Plio-Pleistocene flood basalts and subglacial deposits and upper Pleistocene volcanics. The Tertiary flood basalts are located in the north, northwest and eastern parts of Iceland. They range in age from 3 Ma in the center of Iceland to 13 Ma in the East and 16 Ma at Vestfirðir. The Plio-Pleistocene formation is found adjacent to the neovolcanic zones and at Skagi in Northern Iceland. It consist of hyaloclastites and volcanogenic sediments. The upper Pleistocene formation are hyaloclastites and subaerial basalts that are associated with active rifting and volcanism in the neovolcanic zones and on Snæfellsnes in the last 0.8 Ma (Jóhannesson & Sæmundsson, 1998).

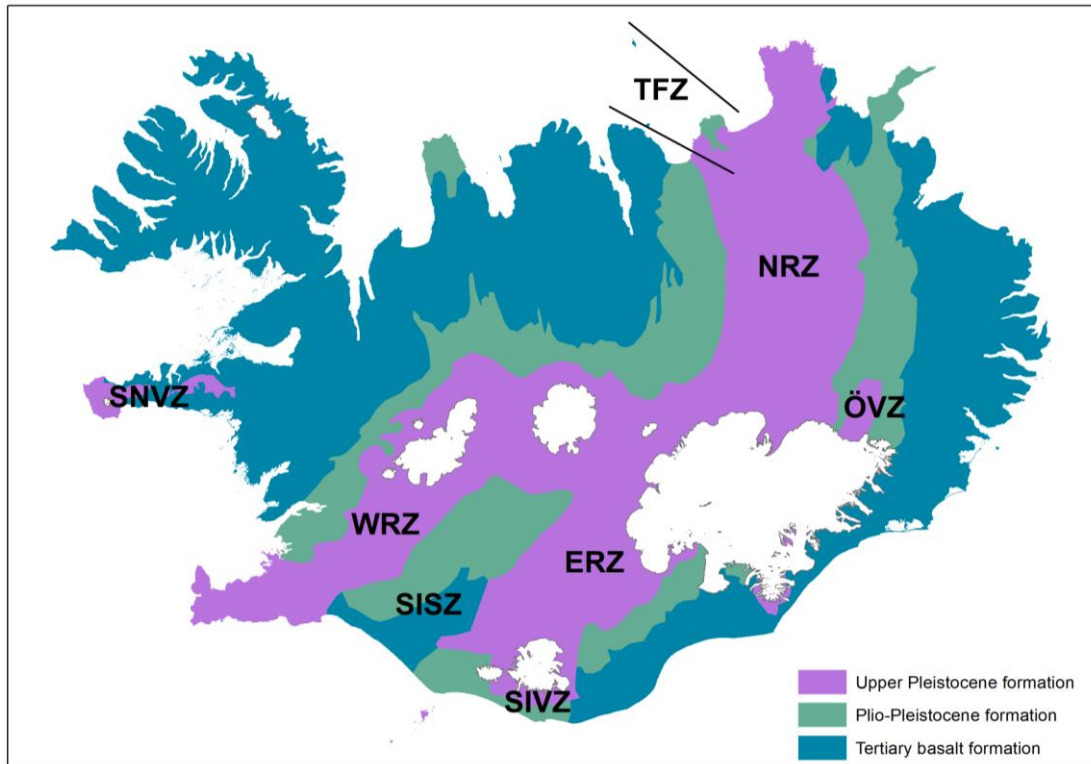


Figure 2: The neovolcanic zones of Iceland. The rift zones are NRZ (Northern Rift Zone), WRZ (Western Rift Zone) and ERZ (Eastern Rift Zone). The volcanic zones are SNVZ (Snæfellsnes Volcanic Zone), SIVZ (South Iceland Volcanic Zone) and ÖVZ (Öræfajökull Volcanic Zone). The transform fault zones are SISZ (South Iceland Seismic Zone) and TFZ (Tjörnes Fracture Zone). Based on Jóhannesson and Sæmundsson (1998)

4 Methods

Data for the maps came from several places. The data base IS 50V, operated by Landmælingar Íslands was used for the Icelandic coastline and glaciers. Data from Náttúrfræðistofnun Íslands about the age of geological formations was also used. In addition, a data base involving published helium isotopes in Icelandic volcanics, glasses and phyrlic lavas, as well as geothermal fluids was constructed from 30 articles, which are shown in Table 1.

Table 1: Articles used to construct the data base

Article	Year	Geothermal			
		Fluids ^a	Glasses ^a	Phenocrysts ^a	Breccia ^a
Kononov & Polak	1975	46			
Polak et al.	1976	10			
Hauksson & Goddard	1981	4			
Torgersen & Jenkins	1982	8			
Condomines et al.	1983		20		
Kurz et al.	1985		19	2	1
Sano et al.	1985	11			
Poreda et al.	1986		3	4	
Hilton et al.	1990	64			
Marty et al.	1991	18			
Poreda et al.	1992	52			
Burnard et al.	1994		6	2	
Hilton et al.	1998	34			
Harrison et al.	1999		2		
Hilton et al.	1999			6	
Breddam et al.	2000		21	8	
Dixon et al.	2000		10	10	
Trieloff et al.	2000		2		
Moreira et al.	2001		7		
Dixon	2003			8	
Ellam & Stuart	2004			5	
Burnard & Harrison	2005		10		
Macpherson et al.	2005		12	13	
Licciardi et al.	2006			22	
Brandon et al.	2007		4	14	
Licciardi et al.	2007			42	
Debaille et al.	2009			5	
Füri et al.	2010	71	78	21	
Peate et al.	2010			16	
Halldórsson et al.	2016		16		

^a: values indicate the numbers of He isotopes data extracted from each reference.

Excel was used to construct the data base, which included 12 columns with different attributes. These attributes were: sample name, phase, area, location, longitude, latitude, R_M/R_A , X-factor, R_C/R_A , concentration of helium, the reference and since not all values had reported values for X-factor and R_C/R_A 1 more column was added that contained the R/R_A value used for analysis in ArcGIS. R_C/R_A was used where it was reported, otherwise R_M/R_A was used. The data base included a total of 707 samples, 318 geothermal fluids, 211 glasses, 177 phenocrysts and 1 breccia (see Appendix).

The constructed data base was made uniform. First coordinates were found for every sample in the data base. To find coordinates the map at ja.is was used along with articles including coordinates of samples taken in same places. Kononov & Polak (1975) presented their results on a map, since no locations were reported ArcGIS was used to calculate the coordinates of the samples. The map from Kononov & Polak (1975) was georeferenced in ArcGIS and a new point layer was drawn on top of the sample sites presented in the study. The coordinates of the new point layer were calculated by using the method Calculate Geometry. Coordinates for all the samples in the data base were calculated to the form decimal degrees.

4.1 Evaluation of the data base and filtering criterion

4.1.1 Air contamination

To recognize air contamination the X-factor is used. To calculate the X-factor the $^4\text{He}/^{20}\text{Ne}$ ratio is measured. It is assumed that all of the neon is of atmospheric derivation. The ratio of $^4\text{He}/^{20}\text{Ne}$ in laboratory air is used for calculations.

$$X = \frac{(^4\text{He}/^{20}\text{Ne})_{\text{measured}}}{(^4\text{He}/^{20}\text{Ne})_{\text{air}}}$$

This correction is valid for mantle and crust samples since the $^4\text{He}/^{20}\text{Ne}$ ratio of the mantle and the crust is many orders of magnitude greater than that of air. For fluid samples different solubility's of helium and neon in water have to be considered. The Bunsen solubility coefficients for neon (β_{Ne}) and helium (β_{He}) are used to account for this, at the temperature and salinity of the water when the atmospheric helium was dissolved.

$$X = \frac{(^4\text{He}/^{20}\text{Ne})_{\text{measured}}}{(^4\text{He}/^{20}\text{Ne})_{\text{air}}} * \frac{\beta_{\text{Ne}}}{\beta_{\text{He}}}$$

The corrected $^3\text{He}/^4\text{He}$ ratio (R_C/R_A) can be calculated when the X-factor is known.

$$R_C/R_A = \frac{(R_M/R_A * X) - 1}{X - 1}$$

The higher the X-factor the less difference between R_M/R_A and R_C/R_A . The X-factor can also be used to calculate the corrected helium concentration ($[\text{He}]_C$), that is related to the measured helium concentration ($[\text{He}]_M$) in the following way (Hilton, 1996).

$$[He]_c = [He]_M \frac{X - 1}{X}$$

It was determined that all samples which had X-factor ≤ 5 were too contaminated considering air-derived helium. Figure 3 shows that for higher X-factor the variability in R_M/R_A increases. Where the X-factor is smaller than 5 almost all samples have R_M/R_A between 1 and 5 R_A . This indicates that samples with X-factor smaller than 5 have been contaminated by air-derived helium. The X-factor was only reported for 247 samples, which is approximately one third of the data base. The 247 samples included 224 geothermal fluids, 20 glasses and only 3 phenocrysts.

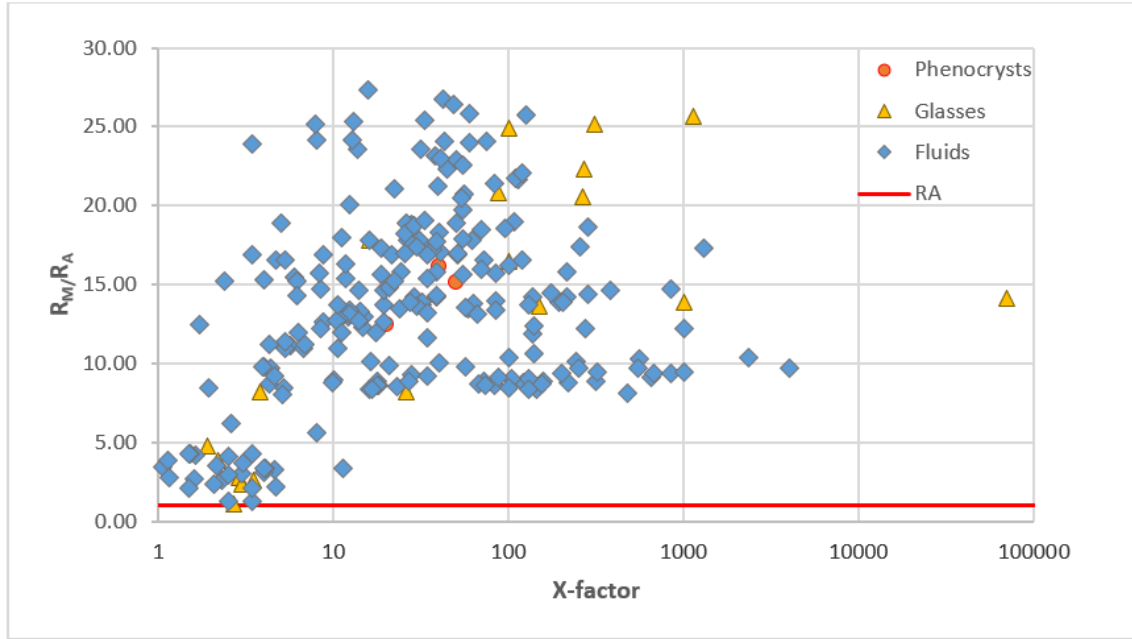


Figure 3: Helium isotope ratios plotted against the X-factor for geothermal fluids, glasses and phenocrysts

4.1.2 Helium concentration

As the X-factor was not reported for all the samples, other methods had to be applied for evaluation. The helium concentration is a factor that can be used to observe air-contamination. Concentration of helium in air and water is low compared to concentrations frequently observed in samples. Since crustal or primordial helium are added components, the higher the helium concentration, the less significant air contamination (Torgersen & Jenkins, 1982). Helium concentrations were plotted against the measured helium isotope ratio, both for glasses (Figure 4) and phenocrysts (Figure 5) to investigate if the helium concentration affected the R_M/R_A . Figure 4 shows more variability in the $^3\text{He}/^4\text{He}$ ratio for higher helium concentration. However $^3\text{He}/^4\text{He}$ ratios close to R_A are observed for both low and high helium concentrations. For phenocryst (Figure 5) variability in the $^3\text{He}/^4\text{He}$ ratio is observed for all concentrations. Due to the great variability in R_M/R_A , for both low and high concentrations, the data was not filtered considering helium concentrations.

Samples from Burnard et al. (1994) were not included in Figure 4 and Figure 5 since there might be an error in how the concentrations are reported. Concentrations are reported in

$\text{cm}^3\text{STP/g} \times 10^{-13}$, which is three orders of magnitude lower than the lowest samples shown in Figure 4 and Figure 5. It is also noted that the detection limit used for helium concentrations in Burnard et al. (1994) is $2 \times 10^{-11} \text{ cm}^3\text{STP/g}$, which is higher than the reported concentrations.

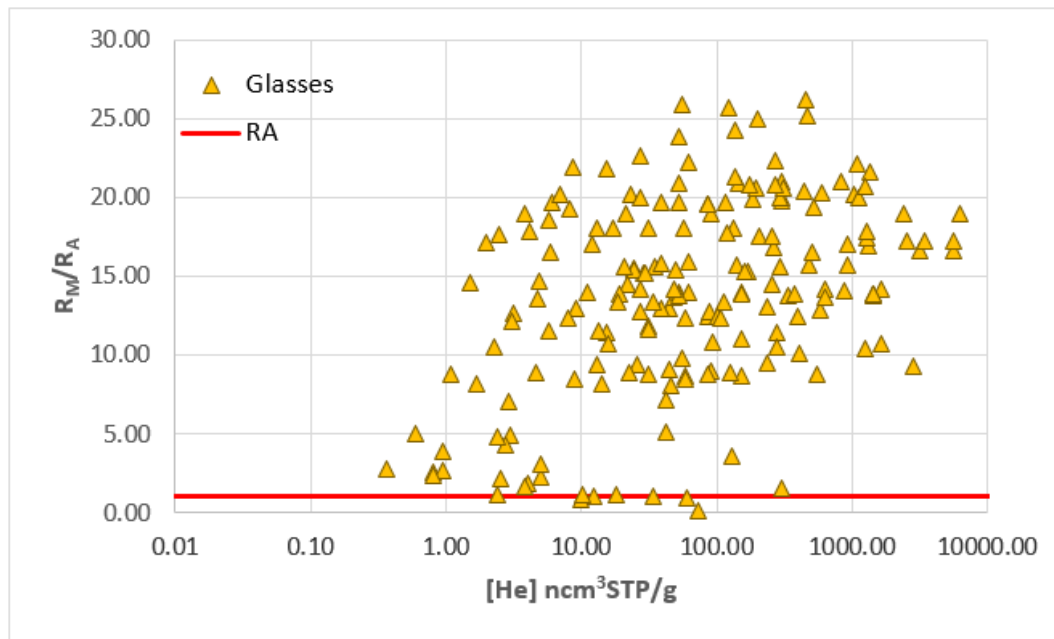


Figure 4: Helium isotope ratios plotted against helium concentrations for volcanic glasses

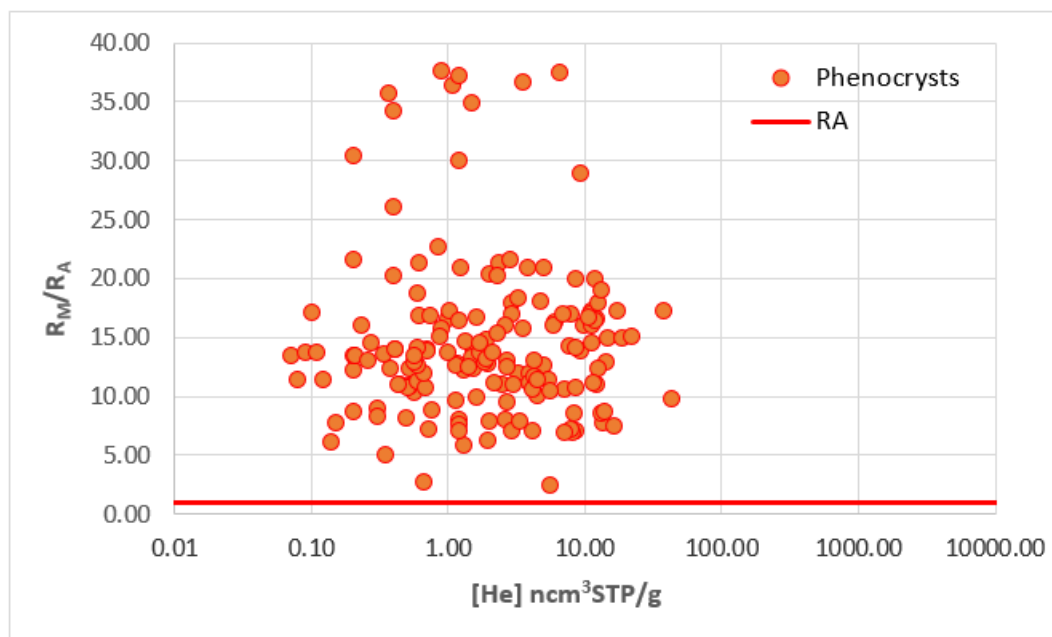


Figure 5: Helium isotope ratios plotted against helium concentrations for phenocrysts

4.1.3 Duplicate samples

For duplicate samples, the sample with the higher helium isotope ratio was used. For example, the sample SK82-13 from Þríhyrningur was measured by Moreira et al. (2001) to

have a ratio of 25.6 R_A and Kurz et al. (1985) to have a ratio of 26.2 R_A . The ratio from Kurz et al. (1985) was included in the final data base.

4.1.4 Samples from the same general region yielding different results

Samples that are significantly lower than other samples in the same general region were also filtered from the data base. For example, at Kverkfjöll $^3\text{He}/^4\text{He}$ ratios of 8-9 R_A are observed. Füri et al. (2010) measured a ratio of 2.27 R_A and Macpherson et al. (2005) measured a ratio of 1.6 R_A at Kverkfjöll, which were not included in the final data base.

4.1.5 Other problems

The location of a few samples was not known with certainty, these samples were not included in the final data base. Following this protocol, the data base decreased to a total of 605 samples, 273 geothermal fluids, 163 glasses, 168 phenocrysts and 1 breccia.

4.2 Methods in ArcGIS

To investigate the distribution of the samples, maps that show the helium isotope ratio (R/R_A) of each sample as a point were made. The data was classified into 8 breaks. Manual breaks were used since the aim was to show how the helium isotope ratio changes with location. Maps were made for each phase and for the combined data, both filtered and unfiltered.

The filtered data was used for interpolation. Interpolation is a method or a mathematical function that estimates the values of cells at locations that lack sampled points. Interpolation is based on spatial dependence, which measures degree of dependence between objects. The two types of interpolation techniques are deterministic and geostatistical. Deterministic techniques create surfaces based on measured points or mathematical formulas. Geostatistical techniques are based on statistics and are used for more advanced surface modeling. The Spatial Analyst extension was used to make the interpolation maps. The Spatial Analyst extension provides tools for spatial data analysis that apply statistical theory and techniques to the modeling of spatially referenced data (Childs, 2004).

Many interpolation methods were executed, those were Spline, Spline with Barriers, Natural Neighbor, IDW, Kriging and Trend. Different methods showed similar results in most cases, except Spline and Trend that showed a very different results from the other methods. It was decided to use the Natural Neighbor method, since it showed good results and it is a relatively simple method.

The Natural Neighbor method can be used for both interpolation and extrapolation. It generally works well with clustered scatter points and the method can efficiently handle large input point data sets. The method is based on a weighted average. Each cell value is determined by using a linear-weighted combination set of sample points. The weight assigned is a function of the distance of an input point from the output cell location. The greater the distance, the less influence the point has on the output value (Childs, 2004).

Interpolation methods do not show values outside the extremities of the data set. So interpolation could be executed for all the country, data outside of Iceland had to be added to the data set. Data points were added around Iceland so interpolation could be done for the whole country. All samples outside of Iceland were given the ratio 5 for R/R_A . These points were located far from the Icelandic coastline so results would only be affected in areas where no sampling had occurred.

Contours were made from the interpolation raster. Contours are used to define a common characteristic along a line. They join locations of equal value to each other (Childs, 2004). The method Contour List was used, since values that contours are drawn for can be chosen with this method. Contours were drawn for the same ratios that were used to make breaks on the distribution maps (7, 9, 12, 14, 17, 20 and 24 R_A). Contour was also drawn for 30 R_A so the highest ratios would be seen on the map.

5 Results

5.1 Geothermal fluids

The distribution of samples for each phase was examined, each phase has its own unique distribution. The geothermal samples (Figure 6) are distributed over most of the country, the distribution is restricted to geothermal areas, both high- and low-temperature areas. Plenty of sampling has been carried out in Vestfirðir. The $^3\text{He}/^4\text{He}$ ratios in Vestfirðir are diverse, showing both low and high ratios. A cluster of samples is located in low-temperature areas in Southern Iceland, where the SISZ and the WRZ merge. This cluster shows high $^3\text{He}/^4\text{He}$ ratios, which decreases to the West throughout the Reykjanes peninsula. Along the Snæfellsnes peninsula $^3\text{He}/^4\text{He}$ ratios seem to increase from the West of Snæfellsnes to the East, with the highest $^3\text{He}/^4\text{He}$ ratio measured at Rauðamelsölkelda. In Borgarfjörður moderately high $^3\text{He}/^4\text{He}$ ratios are measured. Along the NRZ low ratios are measured, the helium isotope ratio seems to increase to the West in northern Iceland and at Borðeyri moderately high $^3\text{He}/^4\text{He}$ ratio is measured. In eastern Iceland sampling has been done at Þveit, Vopnafjörður and Lagarfljót, in all cases low ratios are obtained. In central Iceland high ratios are observed at Köldukvíslarbotnar and Vonarskarð, close to Vatnajökull. Lower ratios are observed in the western part of central Iceland at Hveravellir and Kerlingarfjöll.

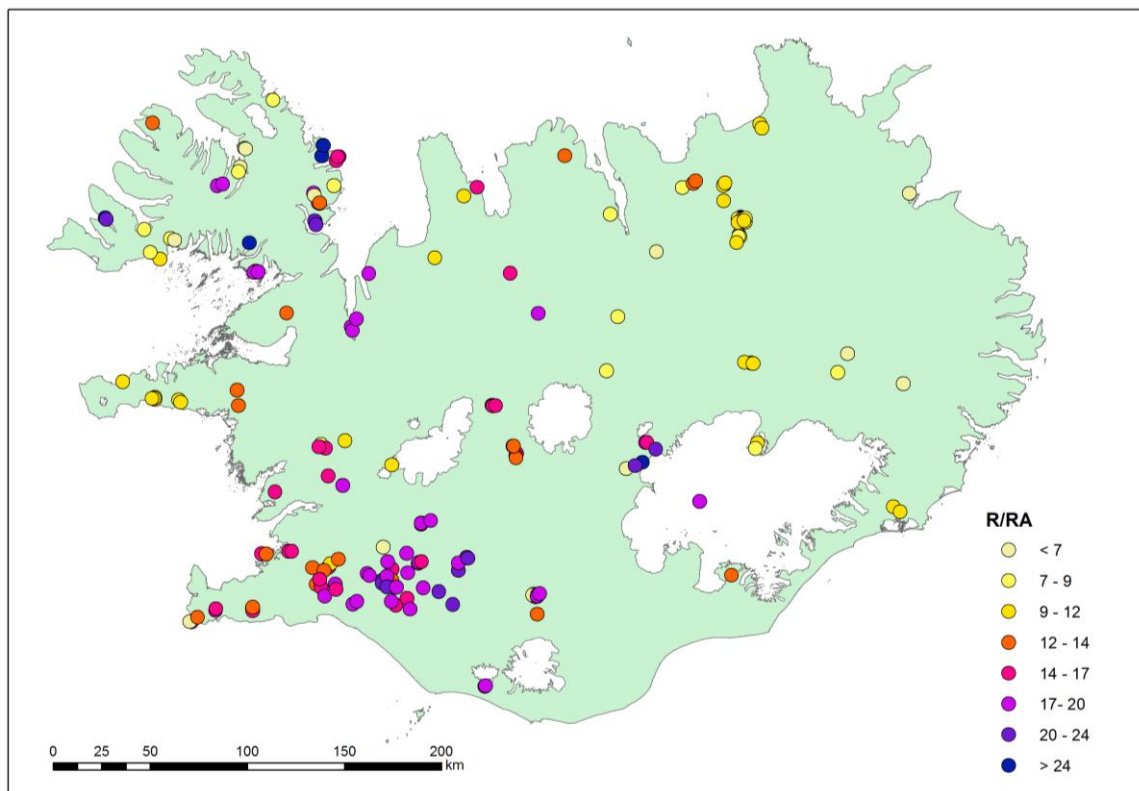


Figure 6: Helium isotope ratios for geothermal fluids

The samples located at the high-temperature area Grímsvötn under the Vatnajökull ice cap were sampled during a jökulhlaup by Hilton et al. (1990). Grímsvötn is drained periodically by a jökulhlaup to the river Skeiðará at the southern ice margin. Two samples were taken at the point of emergence of the river from the glacier during a jökulhlaup. One sample was contaminated but the other one had a reasonably high X-factor and could be used for further analysis. The sample is used to represent the $^3\text{He}/^4\text{He}$ ratio of the Grímsvötn high-temperature area and is located over the geothermal field at Vatnajökull.

5.2 Subglacial lavas

The distribution of glass samples (Figure 7) is confined by the rift and volcanic zones. Most of the samples are located within the rift zones and a few samples are located in the volcanic zones. One sample is located outside of these zones that is an obsidian sample from Pingmúli central volcano in Eastern Iceland. The sample was measured by Condimines et al. (1983) and shows a low $^3\text{He}/^4\text{He}$ ratio, most likely due to air contamination. The glass samples cover most of the rift zones, which each show a distinctive helium isotope ratio. Low ratios are measured in the NRZ, with the exception of higher ratios from Dyngjufjöll Ytri (Breddan et al., 2000; Füri et al. 2010). In the WRZ moderate ratios are observed. In central Iceland high ratios are observed from northwestern Vatnajökull to Arnarbæli between Langjökull and Hofsjökull. In Southern Iceland along the ERZ the samples show bimodal distribution considering the helium isotope ratio. Most of the samples show either high ratios or very low ratios. In Snæfellsnes, at Öraefajökull and Grímsvötn low ratios are measured. These samples along with other low ratio ($\leq 7 R_A$) samples are most likely contaminated by air-derived helium.

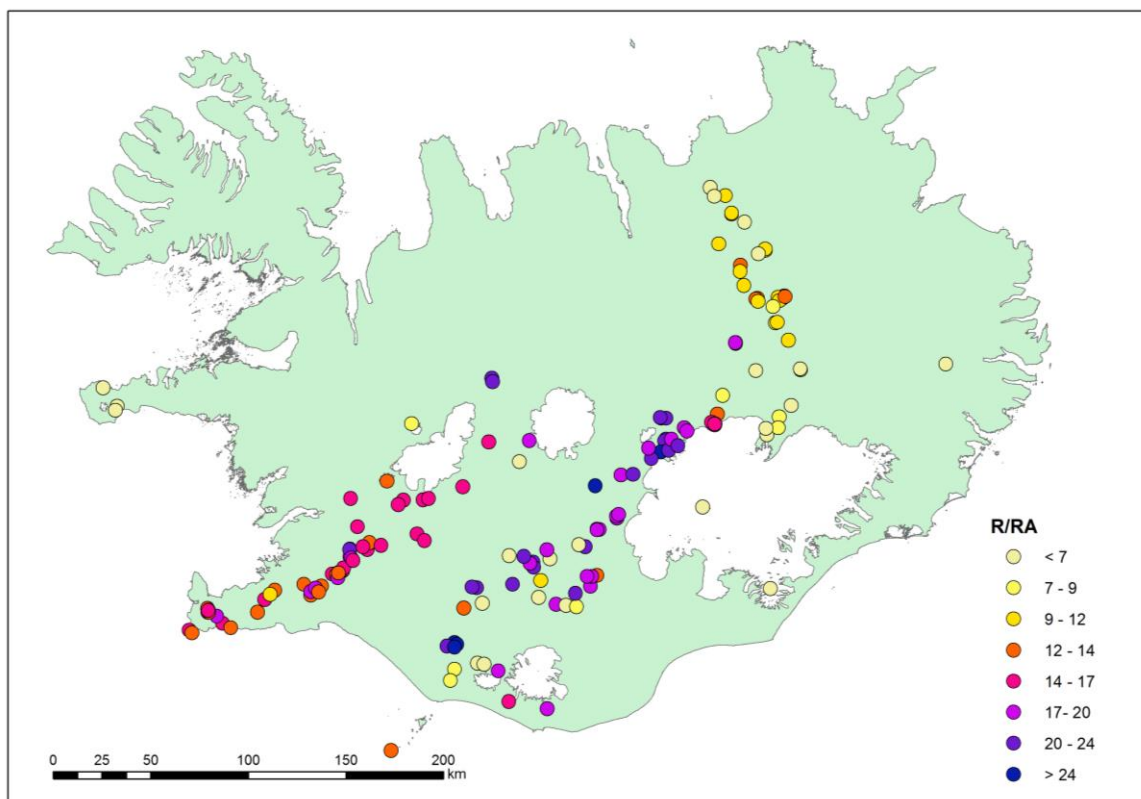


Figure 7: Helium isotope ratios for volcanic glasses

5.3 Phyric lavas

Olivine and few clinopyroxene phenocrysts from phyric lavas have been used to measure the helium isotope ratio. Phenocryst samples (Figure 8) have been sampled in rather restricted areas over the country. Most of the sampling has been carried out in the NRZ and the WRZ. The phenocrysts in the NRZ show, like geothermal fluids and glasses, low ratios, with few exceptions. Samples around Melrakkaslétta measured by Liccardi et al. (2007) show higher ratios than the surrounding samples. Macpherson et al. (2005) also measured high values at Fjallsendi and at Vaðalda. In the WRZ moderate ratios, similar to ratios from glasses and geothermal fluids, are observed. Sampling has been carried out along Snæfellsnes all the way to Bjarnardalsá. The $^3\text{He}/^4\text{He}$ ratio seems to be constant throughout the Snæfellsnes peninsula, but a higher ratio is measured at Bjarnardalsá. Samples in Vestfirðir show the highest ratios measured for phenocrysts, except one sample that shows a very low ratio. The phenocryst samples in Vestfirðir are different from the geothermal fluids in Vestfirðir that showed a big variability in the helium isotope ratio. In Vopnafjörður one sample with moderate $^3\text{He}/^4\text{He}$ ratio was measured by Ellam and Stuart (2004). Peate et al. (2010) sampled phenocrysts in the ÖVZ, these samples show ratios in the MORB range. Finally some sampling took place in Southern Iceland, both around Mýrdals- and Eyjafjallajökull, in Þjórsárdalur and in Vestmannaeyjar and Surtsey. High ratios were measured in Southern Iceland, with lower ratios measured in Vestmannaeyjar and Surtsey.

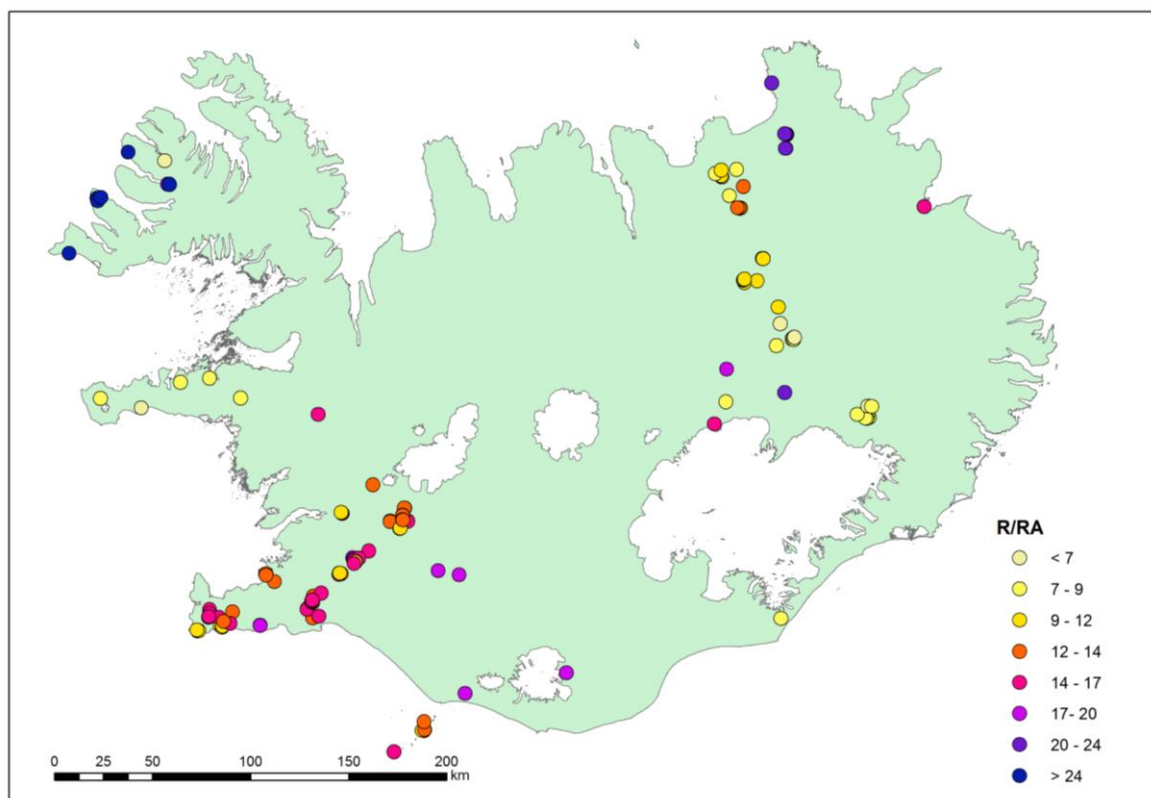


Figure 8: Helium isotope ratios for phenocrysts

5.4 Combined data

Figure 9 shows the combined data. The combination of the data strengthens the distribution of the samples, since different phases have been sampled in different localities. The data density is strongest along the rift zones and through the SISZ. It is fairly strong at the SNVZ, SIVZ and in Vestfirðir. The ÖVZ is mostly covered by Vatnajökull, sampling has been conducted in areas outside of Vatnajökull, but no sampling has been carried out on the glacier itself. This results in poor data density along the ÖVZ. The poorest data density is observed in eastern Iceland. Only few samples have been taken to the east of the NRZ and most of these samples are located at Snæfell in the ÖVZ. The data density is also poor in northern Iceland, with only few samples taken outside of the NRZ. In western Iceland the data density is moderately good. No data is available in the area close to the shore between Mýrdalsjökull and Vatnajökull, since no sampling has been conducted in that area.

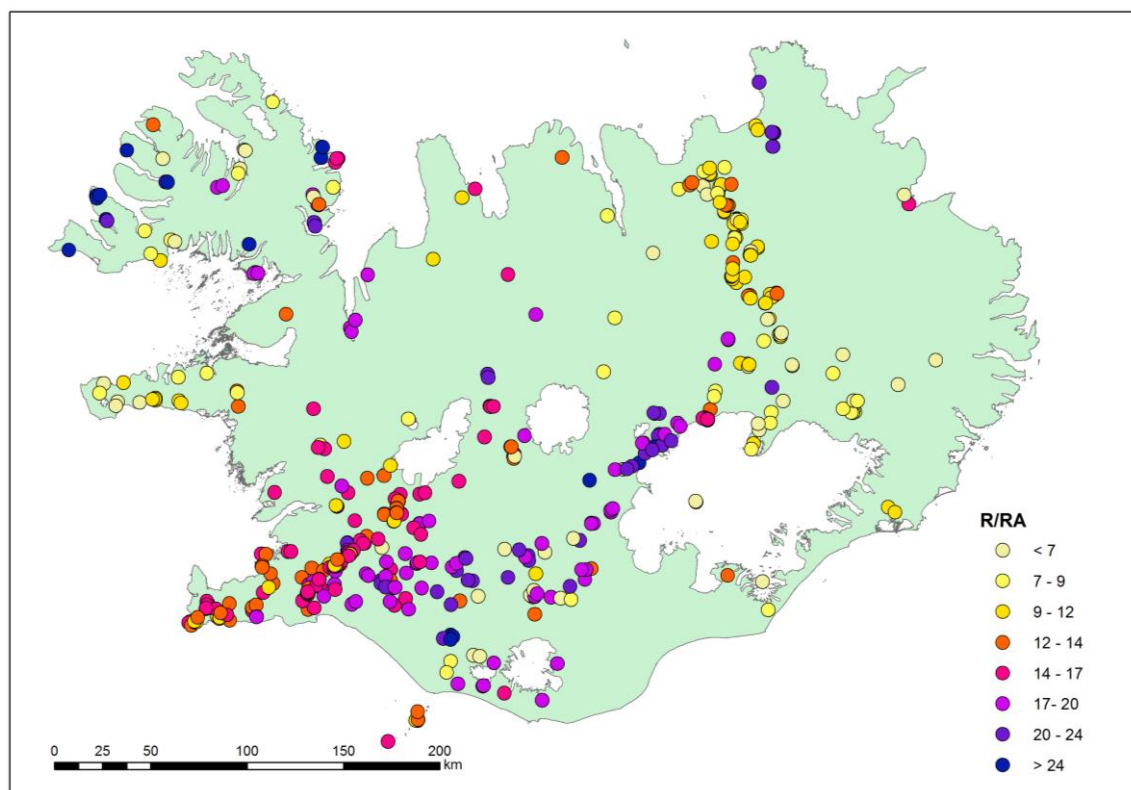


Figure 9: Helium isotope ratios for the combined data

5.5 Filtered data

The data was filtered considering: (1) the X-factor, where it was reported, (2) outliers, both compared to other samples from the same general region and from duplicate measurements and (3) certainty of the location. The filtered data shows clearly the variability in the helium isotope ratio (R/R_A) between different neovolcanic zones (Figure 10). This variability is most obvious in the rift zones. Low ratios in the NRZ, moderate ratios in the WRZ and high ratios in the ERZ, which continue through the SISZ.

The most notable changes in the data after filtering are observed in southern Iceland and at Vestfirðir. In southern Iceland the distribution is no longer bimodal and low ratios have completely disappeared during filtering. In Vestfirðir many low ratio samples have also disappeared due to low X-factor or outliers. Notable changes are observed along the NRZ, in eastern Iceland and along the SNVZ, where low ratio samples have also decreased.

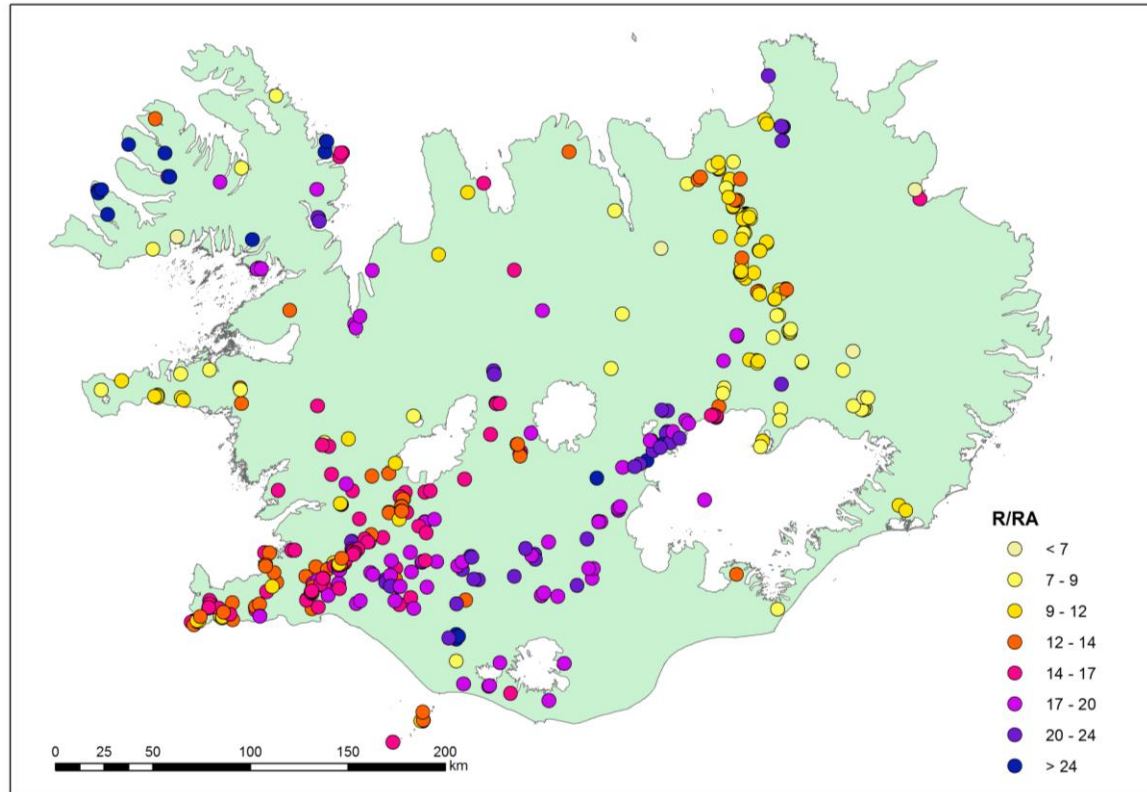


Figure 10: Helium isotope ratios for the filtered data

5.6 Interpolation

The filtered data set was interpolated with the Natural Neighbor method (Figure 11) to estimate the helium isotope ratio where no measurements are available. The dashed lines (Figure 11) define areas where no sampling has occurred, results in these areas should be discounted, since there could be changes in the results if more data was gathered in these areas.

The interpolation shows high isotope ratios in Central Iceland, down the ERZ and through the SISZ. High ratios are also observed at Melrakkaslétta. In Vestfirðir both high and low ratios are observed. Low ratios are observed in Eastern Iceland, at Snæfellsnes and along the NRZ. Moderate ratios occur along the WRZ, in western Iceland and in the northwestern part of Iceland.

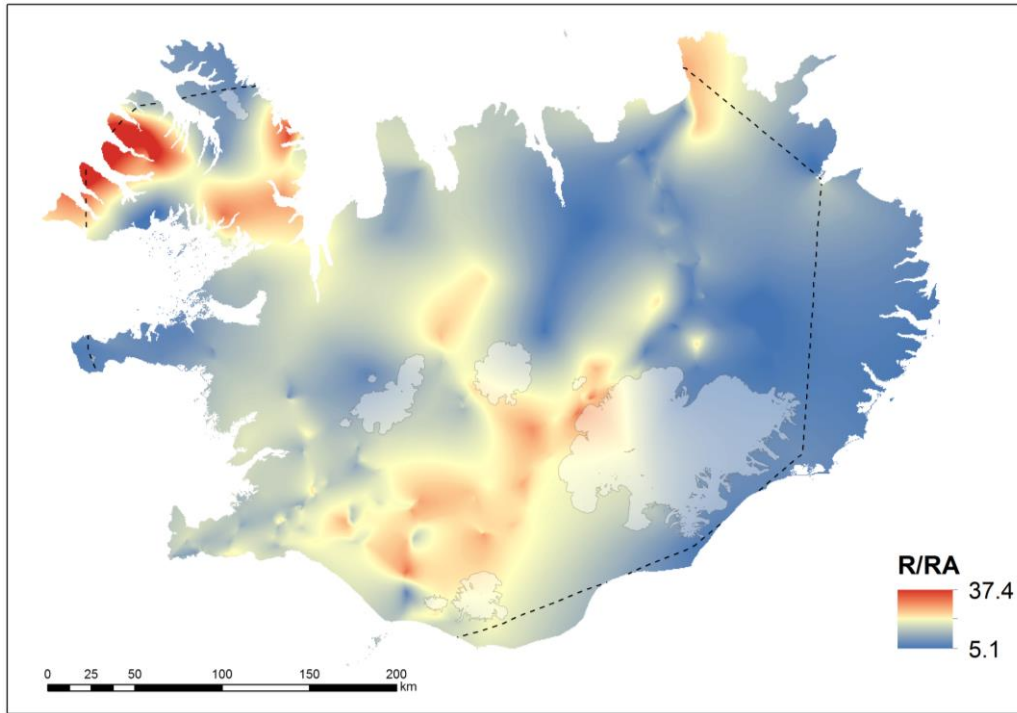


Figure 11: Representative helium isotope ratios calculated with the Natural Neighbor method, areas where no sampling has occurred are shown with the dashed line

Contours were made to connect places with the same helium isotope ratio (Figure 12). The contours show where the same helium isotope ratios are expected. Contours are made from the same filtered data base as Figure 9. Contours were made for 8 different values, 7, 9, 12, 14, 17, 20, 24 and 30 R_A .

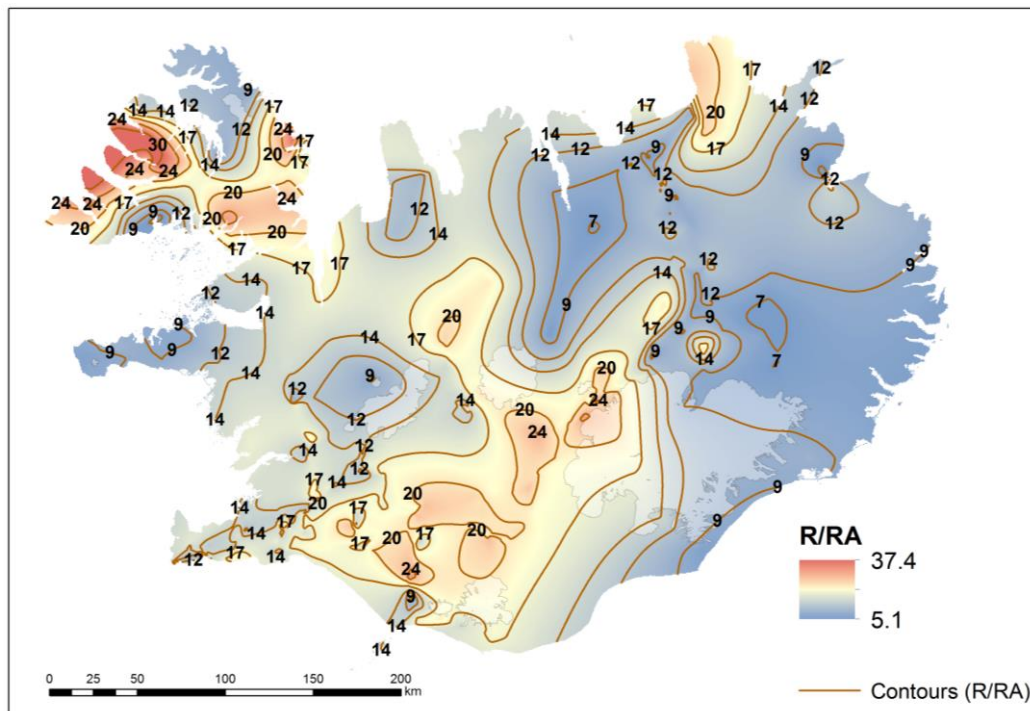


Figure 12: Contours that connect the same helium isotope ratios

6 Discussion

6.1 Regional variability

The data set used in this study shows that the helium isotope ratios (R/R_A) in the whole of Iceland vary between 5.1 and 37.7 R_A and that there is a regional variability in the helium isotope ratio. Below, I will systematically consider the isotope signature for different areas in Iceland, the rift zones, the SISZ, Vestfirðir and the volcanic flank zones.

6.1.1 The active rift zones and the SISZ

Histograms, based on the filtered data, for the rift zones and the SISZ (Figure 13) show a distinctive isotope signature for each zone.

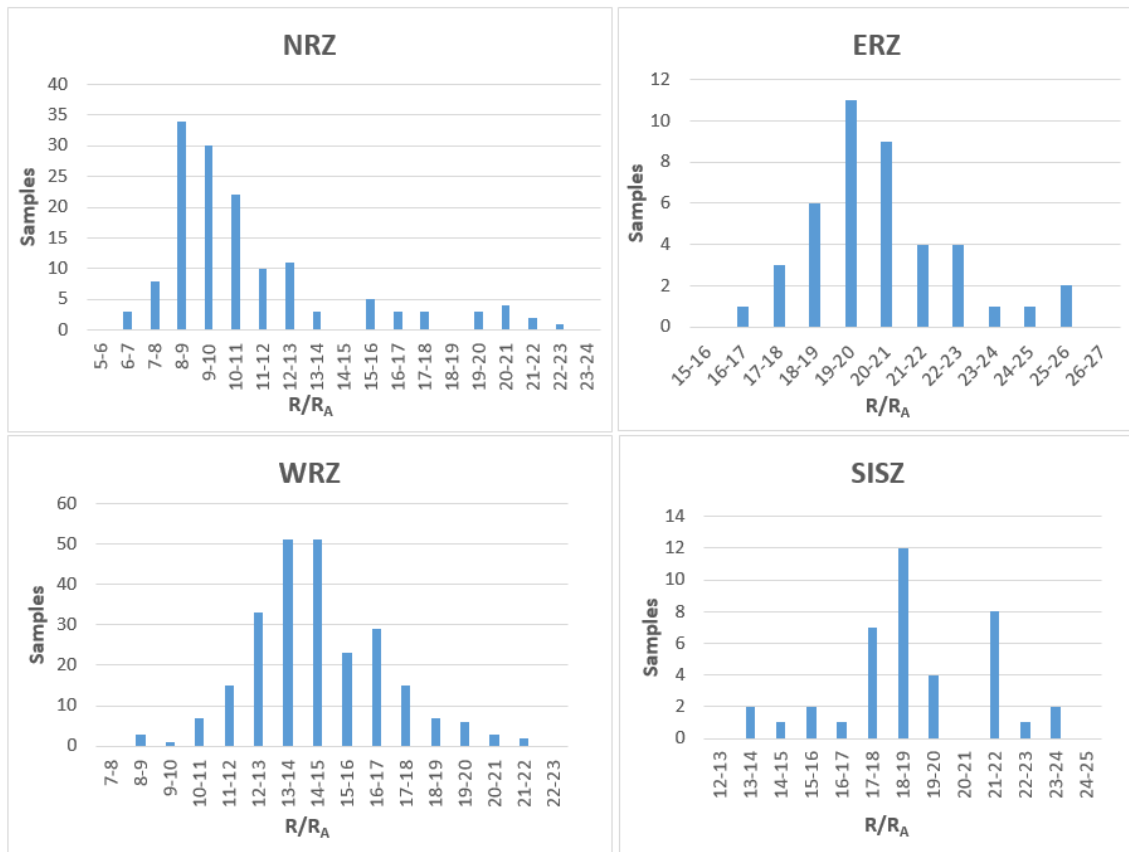


Figure 13: Histograms showing the helium isotope ratios along different rift zones and the SISZ

The histograms show that the NRZ has a range from 7-23 R_A , which can be broken into three smaller ranges. The first one is 6-14 R_A , this range includes the majority of the samples. Distinctive values are from 8 up to 11 R_A . The other two ranges include fewer samples and show higher values, 15-18 R_A and 19-23 R_A . Liccardi et al. (2007) measured

high $^3\text{He}/^4\text{He}$ ratios (20.2-22.7 R_A) in the northernmost part of the NRZ at Hafræfelli, Sandfell and Snarstaðarnúpur. Values between 15 and 18 R_A are measured at Fjallsendi, Kistufell and Dyngjufjöll Ytri (Breddam et al., 2000; Macpherson et al., 2005; Füri et al., 2010), all localities that are close to the mantle plume. The highest ratios of 34.3 R_A and 30.5 R_A measured in olivines and a value of 20.2 R_A measured in clinopyroxene at Vaðalda by Macpherson et al. (2005) are not shown in the histogram.

The ERZ shows higher ratios than the NRZ and has a range from 14-26 R_A , where ratios of 18-21 R_A characterize the area. The WRZ has a range from 9-22 R_A , where ratios from 12-17 R_A characterize the area. These ratios are intermediate between the other two rift zones but significantly higher than MORB values. The SISZ, that connects the ERZ and the WRZ, has a range similar to the ERZ from 13 up to 24 R_A . Characteristic ratios are 18-19 R_A and 21-22 R_A . The distinctive isotope signatures for each rift zone coincide with signatures reported in Kurz et al. (1985).

A high helium plateau (≥ 20 R_A) has been located over central Iceland (Condomines et al., 1983; Kurz et al., 1985; Breddam et al., 2000; Macpherson et al., 2005; Füri et al., 2010). The high ratios in central Iceland continue down the ERZ and through the SISZ (Figure 10). The elevated helium isotope ratios found in lavas along the ERZ may reflect melts generated from the mantle plume being transferred through the ERZ (Breddam et al., 2000) and possibly the SISZ. The high ratios continue to the west from Vatnajökull to near Langjökull. At Langjökull there is a major change in the strike of the rift zone. This change in strike is associated with a change in helium isotope ratios, which start to lower from Langjökull down the WRZ (Kurz et al., 1985).

6.1.2 Vestfirðir

Vestfirðir is characterized among the highest helium isotope ratios worldwide, and considerable variation in the isotope ratio occurs over relatively short (10-50 km) distances (Hilton et al., 1998). The isotope ratio in Vestfirðir varies between 6.2-37.7 R_A . The highest ratio reported for Iceland was measured in late Tertiary basalts from Selárdalur (37.7 R_A) (Hilton et al., 1999). The reasons for the high isotope ratios in Vestfirðir and the off-rift degassing are not clear. Hilton et al. (1990; 1998) suggested that mantle-derived melts that act as a carrier phase for ^3He , are being intruded into the lithosphere under Vestfirðir. Hilton et al. (1998) also suggested that mantle-derived volatiles, trapped within the volcanic pile since eruption, are being released by hydrothermal fluids through chemical alteration and leaching. Poreda et al. (1992) suggested that deep fractures in the basalt have facilitated the transport of gases from the mantle into the crust or that these high ratios mark the plume center at ~9 Ma.

6.1.3 Volcanic flank zones

The off-rift volcanic zones, SNVZ and ÖVZ, are characterized by low helium isotope ratios. The ÖVZ shows MORB values. The SNVZ shows slightly higher ratios, ~9 R_A . The SIVZ which is a continuation of the ERZ (Jakobsson et al., 2008), shows higher ratios than the other volcanic flank zones but slightly lower ratios than the ERZ. The area has a wide range from 8 R_A up to ratios as high as 26.2 R_A , measured at Þríhyrningur (Kurz et al., 1985; Halldórsson et al., 2016).

6.2 Consistency between geothermal fluids, volcanic glasses and phyric lavas

Helium isotope ratios were compared between volcanic glasses, phyric lavas and geothermal fluids. Areas where comparison is possible are the rift zones, NRZ, WRZ and ERZ, and two of the volcanic zones, SNVZ and SIVZ. Previous studies (Hilton et al., 1990; Barry et al., 2013) have shown that geothermal fluids in Iceland have a similar range in most cases in the helium isotope ratio as basalt samples. This suggests that various sample phases are capturing helium from the same mantle source and that there is a close relationship between helium released by hydrothermal activity and helium released by volcanism.

For the western NRZ (Figure 14) it is clearly seen that the $^3\text{He}/^4\text{He}$ ratio decreases to the north. The samples closest to Vatnajökull show considerably higher ratios than other samples along the western NRZ. Geothermal fluids show values from 6 to 12 R_A throughout the zone. Phenocryst and glasses in the northern part of the zone are in most cases consistent with geothermal fluids, showing values up to 14 R_A . Close to Vatnajökull values up to 20 R_A are observed in volcanic glasses and phenocrysts show values up to almost 18 R_A .

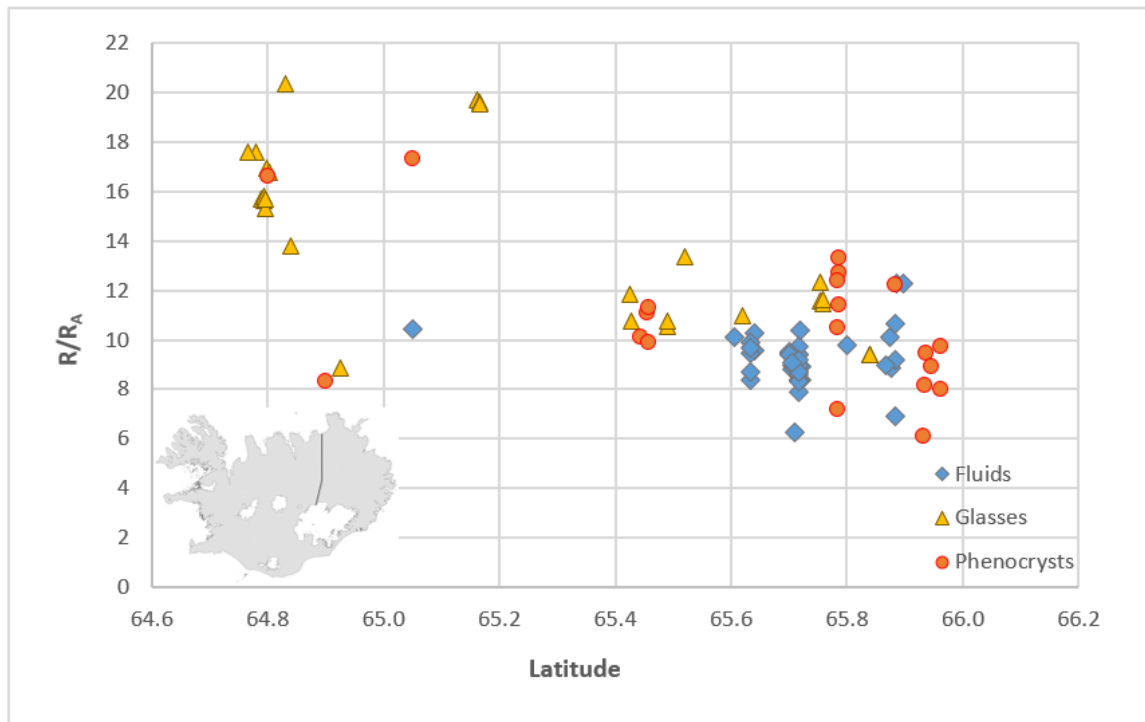


Figure 14: Helium isotope ratios in different sample phases along the western NRZ plotted against latitude

The eastern NRZ (Figure 15) shows $^3\text{He}/^4\text{He}$ ratios between 7 and 13 R_A for almost all the samples. Geothermal fluids show values from 8 to 10 R_A , but glasses and phenocrysts show values up to 13 R_A . There is a good consistency between various phases, with an exception for the northernmost samples where there is a discrepancy between phenocrysts

and geothermal fluids. The northernmost phenocrysts show ratios between 20 and 23 R_A , while fluids show values of 10 R_A .

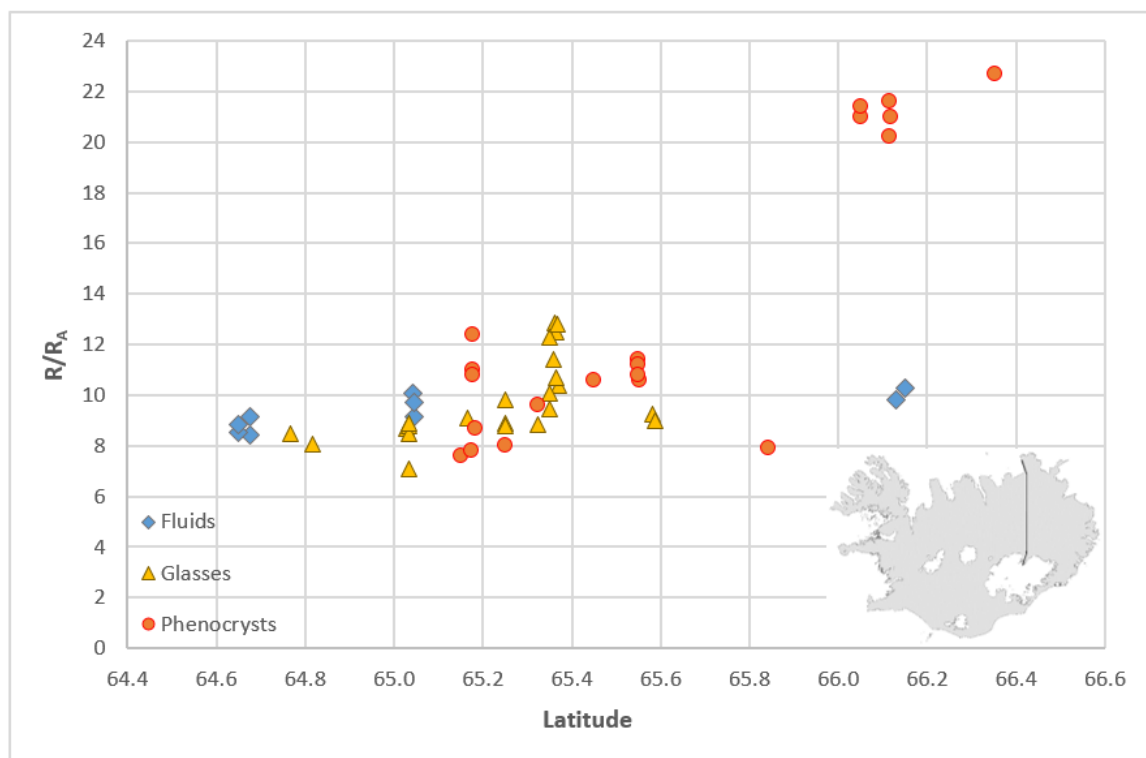


Figure 15: Helium isotope ratios in different sample phases along the eastern NRZ plotted against latitude

Geothermal fluids correspond well to volcanic glasses and phenocrysts along the WRZ (Figure 16). An exception to that is seen in the easternmost part of the zone, where glass samples show higher values than geothermal fluids. Geothermal fluids from the SISZ are also plotted on Figure 16. Some of the fluids from the SISZ are consistent with geothermal fluids from the WRZ. However, the highest helium isotope ratios reported from the SISZ are considerably higher than ratios from the WRZ. It is also noted that the highest isotope ratios for geothermal fluids in the WRZ are measured at longitudes where the WRZ and SISZ merge.

Along the ERZ (Figure 17) there is an excellent consistency between volcanic glasses and geothermal fluids over a range of 16-26 R_A . The geothermal fluids from the SISZ also show a good consistency with samples from the ERZ, except for the lowest ratios measured from the SISZ. Along the SIVZ lower helium isotope ratios are observed, the samples cover a large range but various phases seem to overlap each other. Glass samples from Þríhryningur show much higher ratios ($\sim 26 R_A$) than other samples from the SIVZ and are therefore not consistent with other samples.

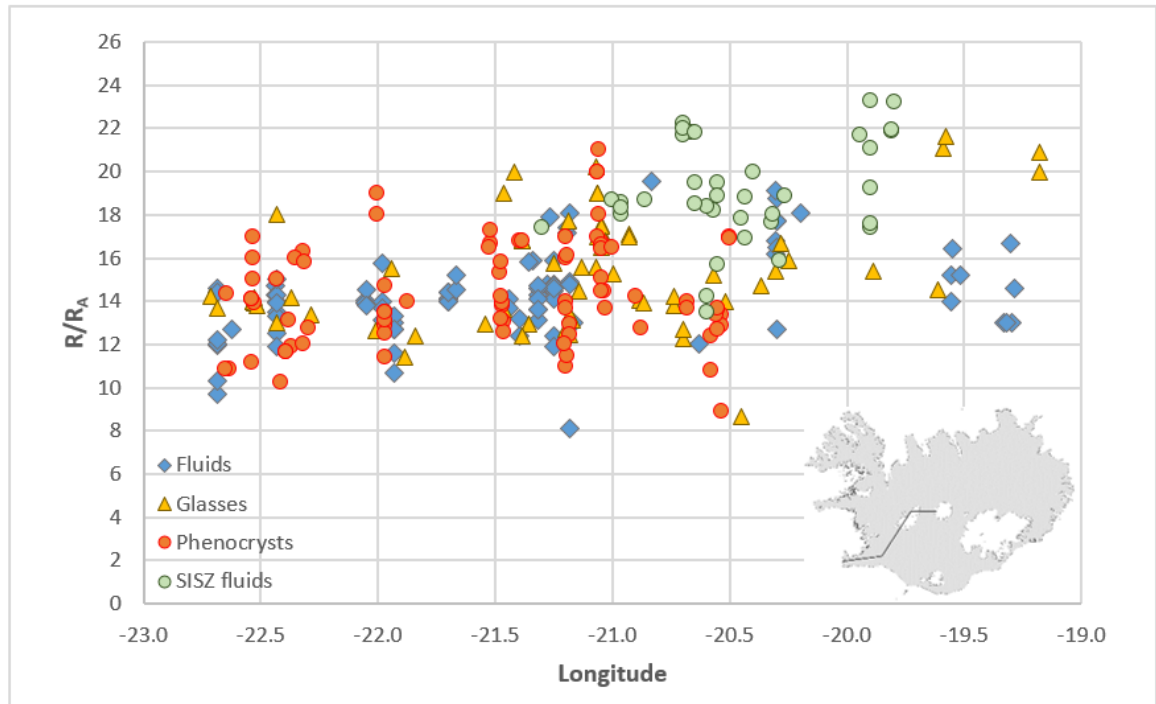


Figure 16: Helium isotope ratios in different sample phases along the WRZ and geothermal fluids from the SISZ plotted against longitude

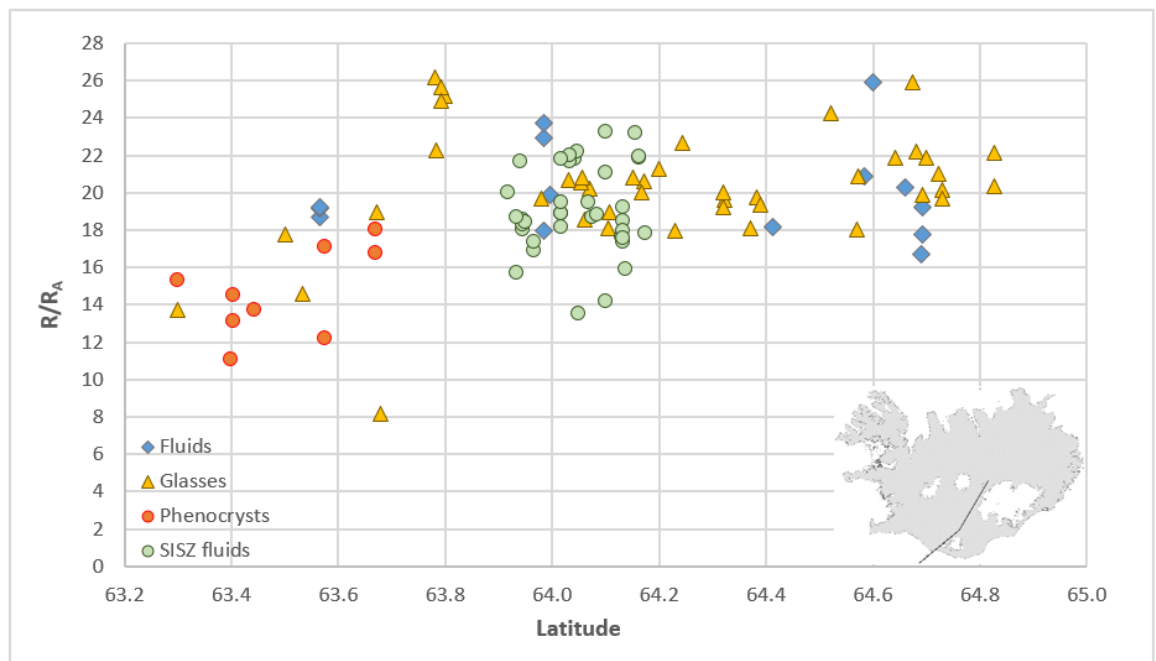


Figure 17: Helium isotope ratios in different sample phases along the ERZ and the SISZ and geothermal fluids from the SISZ plotted against latitude

Phenocrysts and geothermal fluids along the SNVZ (Figure 18) overlap each other. Helium isotope ratios seem to rise to the east for geothermal fluids, but they are consistent through the peninsula for phenocrysts. Therefore, there is a discrepancy between geothermal fluids and phenocrysts at the eastern part of the peninsula.

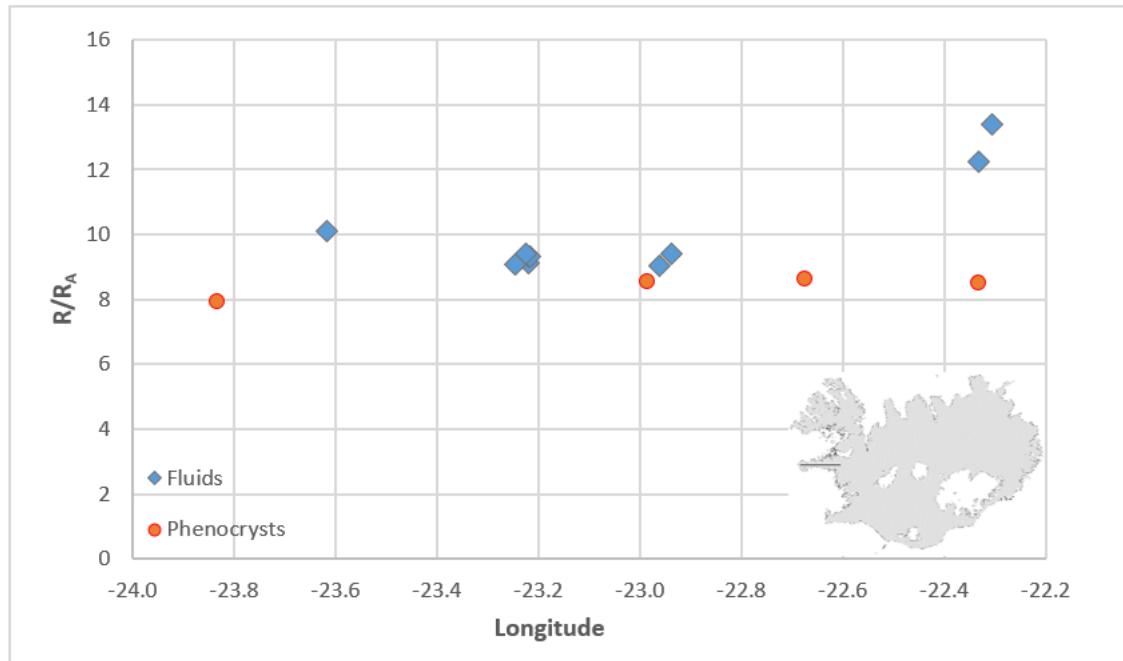


Figure 18: Helium isotope ratios in different sample phases along the SNVZ plotted against longitude

Overall there seems to be a consistency between geothermal fluids, volcanic glasses and phenocrysts, with some exceptions at the NRZ and the SNVZ, where there is a discrepancy between phenocrysts and geothermal fluids. The overall good consistency indicates that helium is coming from the same mantle source for various phases (Barry et al., 2013).

6.3 Comparison with geophysical data

A number of geological properties are most anomalous in central Iceland, over northwest Vatnajökull. These properties include eruption rates, elevation, geoid, seismic velocity and gravity. It is assumed that the center of the mantle plume lies under this region. High helium isotope ratios that are observed in central Iceland are consistent with these properties (Kurz et al., 1985). The maximum seismic velocity (-4.2%) and gravity deviation (-55 mGal) occur over the northwestern part of Vatnajökull (Breddam et al., 2000). A low-velocity anomaly is located in the upper 400 km beneath central Iceland and has been described by many investigators (e.g. Tryggvason et al., 1983; Wolfe et al., 1997; Bijwaard & Spakman, 1999; Bjarnason, 2008). Seismic data shows a cylindrical zone, with a 150 km radius, of low P- and S-wave velocities, this zone extends from 100 km to at least 400 km depth below central Iceland. (Wolfe et al., 1997). The low-velocity anomaly may be rooted deeper, even in the lower mantle (Breddam et al., 2000). The Bouguer gravity anomaly (Figure 19) corresponds well with the high helium plateau in central Iceland. The gravity anomaly differs from the high helium plateau since it does not continue down the ERZ.

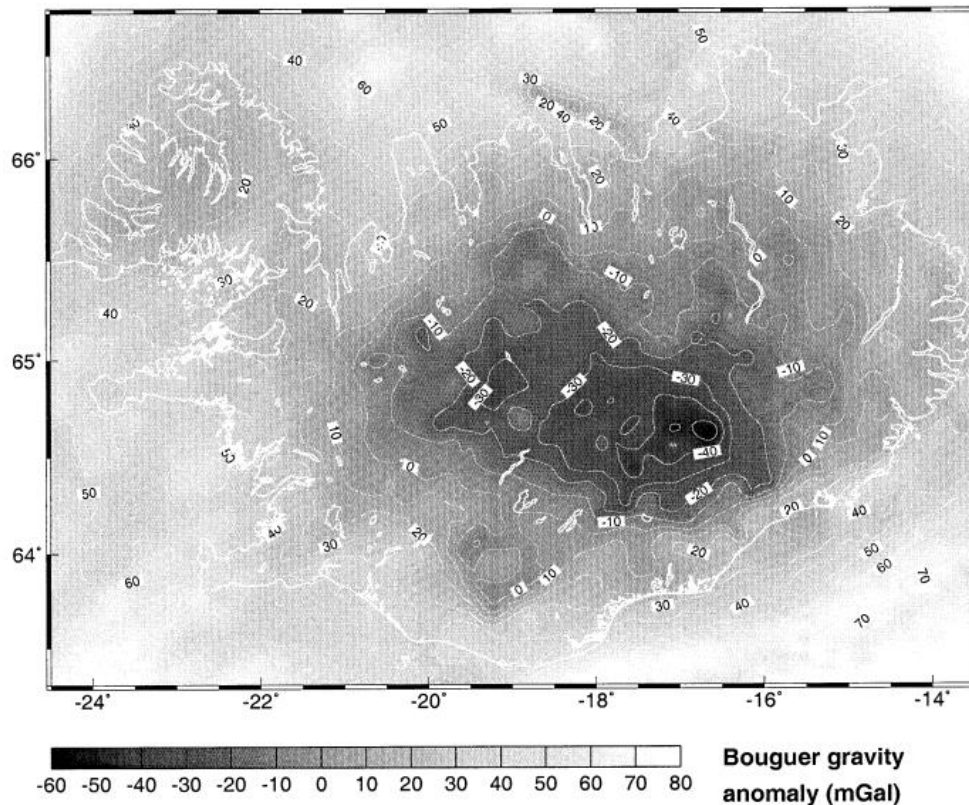


Figure 19: The Bouguer gravity anomaly over Iceland (Darbyshire et al., 2000)

Seismic and gravity measurements have been used to provide a model of the crustal thickness in Iceland. The results of these studies have been interpreted in the way that the thickest crust (~40 km) lies above the center of the mantle plume. Thick crust (~35 km) is also found in Eastern Iceland. The crust thins away from the plume center in other areas and the thinnest crust (≤ 20 km) is located in the far southwest of Iceland and in the northern part of the NRZ (Darbyshire et al., 2000). This interpretation coincides with helium isotope ratios, but has been questioned by Bjarnason and Schmeling (2009) which estimated the average crustal thickness of Iceland to be 25-26 km, using shear waves. They argue that the thickest crust is under eastern Iceland (29-32 km) and Vestfirðir (29 km) and the thinnest part of the crust lies above the mantle plume and in the WRZ (19 km). This crustal thickness is supported by dynamic crust formation models that show a differential flow within the lower crust, that causes crustal material accreted in the central emplacement zone to move sideways with a higher velocity than the spreading velocity.

Bjarnason & Schmeling (2009) also estimated the thickness of the lithosphere to be thinnest below central Iceland and the NRZ (20 km). Under the WRZ and the western part of central Iceland the lithosphere is 30-35 km. The 40-km-deep seismic discontinuity under central Iceland measured by Darbyshire et al. (2000) can then be interpreted as the lithosphere-asthenosphere boundary or a reflector within the mantle asthenosphere. Guðfinnsson (2010) suggested that the 40-km-deep seismic discontinuity is a transition zone in the mantle where spinel peridotite transforms into plagioclase peridotite. The thickness of the lithosphere increases to 55-65 km under Vestfirðir and under eastern Iceland the thickest lithosphere is measured, which is minimum 100 km thick. The thick lithosphere under eastern Iceland is most likely due to an age unconformity that exist between the crust and the mantle under eastern Iceland (Bjarnason & Schmeling, 2009).

6.4 Implications for the Iceland plume structure

The high helium isotope ratios measured in Iceland imply that the source of the Icelandic mantle plume is an undegassed, deep mantle reservoir, whereas the MORB source is a degassed, upper mantle (Moreira et al., 2001). He-Ne systematics from the Icelandic neovolcanic zones suggest a binary mixing between two endmembers, one with a isotope signature similar to depleted MORB-mantle and the other with a more primordial isotope composition (Dixon, 2003; Füri et al., 2010). Local geophysical anomalies, both seismic velocity and gravity anomalies, coincide with the high helium plateau in central Iceland. This suggests that the lateral distribution of plume material is being outlined by helium isotope ratios and that the focus of the mantle upwelling is located in central Iceland (Breddam et al., 2000).

The high helium isotope ratios reported from Vestfirðir and the thick crust beneath the area can also be used to make interpretations about the mantle plume. One explanation for the thick crust under Vestfirðir is that the center of the mantle plume was once located at Vestfirðir. GPS measurements do not support this explanation and suggest that the center of the mantle plume was previously located in Dalasýsla and before that in Breiðafjörður, south to Vestfirðir and the Greenland-Iceland ridge (Bjarnason, 2013). However, the Greenland-Iceland ridge is not well constrained considering plate spreading models and the fixed Pacific hot spot frame (Bjarnason, 2008). The high helium isotope ratios in Vestfirðir support that the center of the mantle plume was once located at Vestfirðir, since OIB values for the $^3\text{He}/^4\text{He}$ ratio indicate that the mantle source is an undegassed lower mantle. The low isotope ratios observed at Snæfellsnes also support this theory. The isotope ratio at Snæfellsnes is characterized by MORB values, which indicate that the mantle source at Snæfellsnes is a degassed, upper mantle.

7 Conclusions

A data base for helium isotopes, that included 707 samples, was compiled for this study. Filtering of the data showed that many samples were not suitable for analysis, due to contamination or lack of information about locality of the sample. A total of 102 samples were filtered from the data base, before spatial analysis were executed.

Helium isotope ratios in the whole of Iceland vary from 5.1 to 37.7 R_A . The highest ratios are measured in the older part of Iceland at Vestfirðir. Within the neovolcanic zones the highest ratios are measured over northwestern Vatnajökull, where the mantle plume is located. The rift zones are characterized by distinctive helium signatures: 8-11 R_A in the NRZ, 12-17 R_A in the WRZ and 18-21 R_A in the ERZ. The SISZ is characterized by ratios between 18 and 19 R_A , which is similar to the ERZ and slightly higher than the WRZ. The off-rift volcanic zones, SNVZ and ÖVZ, show ratios similar to MORB values. The SIVZ, that is a continuation of the ERZ, shows higher ratios than the other off-rift volcanic zones but lower values than the ERZ. There is a good consistency between various phases, which suggests that helium is coming from the same mantle source for various phases.

A high helium plateau ($\geq 20 R_A$) is located in central Iceland. This plateau correlates with geophysical measurements, both seismic velocity and gravity measurements. The high helium isotope ratios are thought to indicate that the source of the mantle plume is an undegassed, deep mantle source and the plateau is thought to outline the lateral distribution of plume material. The high helium isotope ratios and the thick crust at Vestfirðir indicate that the center of the mantle plume was once located there.

References

- Barry P. H., Hilton D. R., Fischer T. P., de Moor J. M., Mangasini F. & Ramirez C. (2013) Helium and carbon isotope systematics of cold “mazuku” CO₂ vents and hydrothermal gases and fluids from Rungwe Volcanic Province, southern Tanzania. *Chem. Geol.* **339**, 141-156.
- Bijwaard H. & Spakman W. (1999) Tomographic evidence for a narrow whole mantle plume below Iceland. *Earth Planet. Sci. Lett.* **166**, 121–126.
- Bjarnason I. Þ. (2008) An Iceland hotspot saga. *Jökull* **58**, 3-16.
- Bjarnason I. Þ. (2013). *Jarðeðlisfræðilegur samanburður a tertíer beltum Austurlands og Vestfjarða og slóð heita reitsins á Íslandi og nágrenni*. Paper presented at Autumn Congress of the Geological Society of Iceland, Reykjavík.
- Brandon A. D., Graham D. W., Waight T. & Gautason B. (2007) ¹⁸⁶Os and ¹⁸⁷Os enrichments and high-³He/⁴He sources in the Earth’s mantle: evidence from Icelandic picrites. *Geochim. Cosmochim. Acta* **71**(18), 4570–4591.
- Breddam K., Kurz M. D. & Storey M. (2000) Mapping out the conduit of the Iceland mantle plume with helium isotopes. *Earth Planet. Sci. Lett.* **176**(1), 45–55.
- Burnard P. & Harrison D. (2005) Argon isotope constraints on modification of oxygen isotopes in Iceland Basalts by surficial processes. *Chem. Geol.* **216**, 143-156.
- Burnard P. G., Stuart F. M., Turner G. & Óskarsson N. (1994) Air contamination of basaltic magmas: implications for high ³He/⁴He mantle Ar isotopic composition. *J. Geophys. Res. – Sol. Earth* **99**(B9), 17709–17715.
- Childs C. (2004) Interpolating surfaces in ArcGIS Spatial Analyst. *ArcUser* **3**, 32-35.
- Condomines M., Grönvold K., Hooker P. J., Muehlenbachs K., O’Nions R. K., Óskarsson N. & Oxburgh E. R. (1983) Helium, oxygen, strontium and neodymium isotopic relationships in Icelandic volcanics. *Earth Planet. Sci. Lett.* **66**(1–3), 125–136.
- Darbyshire F. A., White R. S. & Priestley K. F. (2000) Structure of the crust and uppermost mantle of Iceland from a combined seismic and gravity study. *Earth Planet. Sci. Lett.* **181**(3), 409-428.
- Debaille V., Trønnes R. G., Brandon A. D., Waight T. E., Graham D.W. & Lee C. A. (2009) Primitive off-rift basalts from Iceland and Jan Mayen: Os-isotopic evidence for a mantle source containing enriched subcontinental lithosphere. *Geochim. Cosmochim. Acta* **73**, 3423-3449.

- Dixon E. T. (2003) Interpretation of helium and neon isotopic heterogeneity in Icelandic basalts. *Earth Planet. Sci. Lett.* **206**(1–2), 83–99.
- Dixon E. T., Honda M., McDougall I., Campbell I. H. & Sigurdsson I. (2000) Preservation of nearsolar neon isotopic ratios in Icelandic basalts. *Earth Planet. Sci. Lett.* **180**(3–4), 309–324.
- Eason D. E., Sinton J. M., Grönvold K. & Kurz M. D. (2015) Effects of deglaciation on the petrology and eruptive history of the Western Volcanic Zone, Iceland. *Bull. Volcanol.* **77**(47) 27 pp.
- Einarsson P. (2008) Plate boundaries, rifts and transforms in Iceland. *Jökull* **58**, 35–58.
- Ellam R. M. & Stuart F. M. (2004) Coherent He–Nd–Sr isotope trends in high $^3\text{He}/^4\text{He}$ basalts: implications for a common reservoir, mantle heterogeneity and convection. *Earth Planet. Sci. Lett.* **228**(3–4), 511–523.
- Frost B. R. & Frost C. D. (2014) *Igneous and Metamorphic Petrology*. New York: Cambridge University Press.
- Füri E., Hilton D. R., Halldórsson S. A., Barry P. H., Hahn D., Fischer T. P. & Grönvold K. (2010) Apparent decoupling of the He and Ne isotope systematics of the Icelandic mantle: The role of He depletion, melt mixing, degassing fractionation and air interaction. *Geochim. Cosmochim. Acta* **74**, 3307–3332.
- Gautheron C. & Moreira M. (2002) Helium signature of the subcontinental lithospheric mantle. *Earth Planet. Sci. Lett.* **199**, 39–47.
- Graham D. W. (2002) Noble gas isotope geochemistry of mid-ocean ridge and ocean island basalts: characterization of mantle source reservoirs. In *Noble Gases in Geochemistry and Cosmochemistry*, vol. 47 (eds. D. Porcelli, C. Ballentine and R. Wieler), pp. 247–317. Rev. Mineral. Geochem. Mineral. Soc. Am., Washington DC.
- Guðfinnsson G. H. (2010). *Stafar endurkastsfloður á um 40 km dýpi undir Íslandi af fasabreytingum í möttli?* Paper presented at Autumn Congress of the Geological Society of Iceland, Reykjavík.
- Guðmundsson Á. (2000) Dynamics of volcanic systems in Iceland: Example of tectonism and volcanism at juxtaposed hot spot and mid-ocean ridge Systems. *Annu. Rev. Earth Planet. Sci.* **28**, 107–140.
- Halldórsson S. A., Hilton D. R., Barry P. H., Füri E. & Grönvold K. (2016) Recycling of crustal material by the Iceland mantle plume: New evidence from nitrogen elemental and isotope systematics of subglacial basalts. *Geochim. Cosmochim. Acta* **176**, 206–226.
- Harrison D., Burnard P. & Turner G. (1999) Noble gas behaviour and composition in the mantle: constraints from the Iceland Plume. *Earth Planet. Sci. Lett.* **171**(2), 199–207.

- Hauksson E. & Goddard J. B. (1981) Radon earthquake precursor studies in Iceland. *J. Geophys. Res.* **86**, 7037-7054.
- Hilton D. R. (1996) The helium and carbon isotope systematics of a continental geothermal system; results from monitoring studies at Long Valley Caldera (California, U.S.A.). *Chem. Geol.* **127**(4), 269-295.
- Hilton D. R., Grönvold K., O’Nions R. K. & Oxburgh E. R. (1990) Regional distribution of ^3He anomalies in the Icelandic crust. *Chem. Geol.* **88**(1–2), 53–67.
- Hilton D. R., Grönvold K., Sveinbjörnsdóttir A. E. & Hammerschmidt K. (1998) Helium isotope evidence for off-axis degassing of the Icelandic hotspot. *Chem. Geol.* **149**(3–4), 173–187, *Earth Planet. Sci. Lett.* **173**(1–2), 53–60.
- Hilton D. R., Grönvold K., Macpherson C. G. & Castillo P. R. (1999) Extreme $^3\text{He}/^4\text{He}$ ratios in northwest Iceland: constraining the common component in mantle plumes. *Earth Planet. Sci. Lett.* **173**(1–2), 53–60.
- Jakobsson S. P., Jónasson K. & Sigurðsson I. A. (2008) The three igneous rock series of Iceland. *Jökull* **58**, 117-138.
- Jóhannesson H. & Sæmundsson K. (1998). *Geological map of Iceland*. Bedrock geology, scale 1:500.000. Reykjavík: Náttúrufræðistofnun Íslands (2nd edition).
- Kononov V. I. & Polak B. G. (1975) Indicators of abyssal heat recharge of recent hydrothermal phenomena. *Proc. 2nd United Nations Symposium on the Development and Use of Geothermal Resources.* **2**, 767-773.
- Kurz M. D., Jenkins W. J. & Hart S. R. (1982) Helium isotopic systematics of oceanic islands and mantle heterogeneity. *Nature.* **297**, 43-47.
- Kurz M. D., Meyer P. S. & Sigurðsson H. (1985) Helium isotopic systematics within the neovolcanic zones of Iceland. *Earth Planet. Sci. Lett.* **74**(4), 291–305.
- Licciardi J. M., Kurz M. D. & Curtice J. M. (2006) Cosmogenic ^3He production rates from Holocene lava flows in Iceland. *Earth Planet. Sci. Lett.* **246**, 251-264.
- Licciardi J. M., Kurz M. D. & Curtice J. M. (2007) Glacial and volcanic history of Icelandic table mountains from cosmogenic ^3He exposure ages. *Quat. Sci. Rev.* **26**(11–12), 1529–1546.
- Macpherson C. G., Hilton D. R., Day J. M. D., Lowry D. & Grönvold K. (2005a) High- $^3\text{He}/^4\text{He}$, depleted mantle and low- $\delta^{18}\text{O}$, recycled oceanic lithosphere in the source of central Iceland magmatism. *Earth Planet. Sci. Lett.* **233**(3–4), 411–427.
- Marty B., Gunnlaugsson E., Jambon A., Óskarsson N., Ozima M., Pineau F. & Torssander P. (1991) Gas geochemistry of geothermal fluids, the Hengill Area, southwest rift zone of Iceland. *Chem. Geol.* **91**(3), 207–225.

- Moreira M., Breddam K., Curtice J. & Kurz M. D. (2001) Solar neon in the Icelandic mantle: new evidence for an undegassed lower mantle. *Earth Planet. Sci. Lett.* **185**(1–2), 15–23.
- Mukhopadhyay S. (2012) Early differentiation and volatile accretion recorded in deep-mantle neon and xenon *Nature* **486**, 101–104.
- Peate D. W., Breddam K., Baker J. A., Kurz M. D., Barker A. K., Prestvik T., Grassineau N. & Skovgaard C. (2010) Compositional Characteristics and Spatial Distribution of Enriched Icelandic Mantle Components. *J. Petrology* **51**(7), 1447–1475.
- Petrucchi R. H., Herring F. G., Madura J. F. & Bissonnette C. (2011) *General chemistry Principles and Modern Applications* (10th edition). Toronto, Ontario: Pearson Canada Inc.
- Polak G., Kononov I., Tolstikhin I., Mamyrin B. A. & Khabarin L. V. (1976) The helium isotopes in thermal fluids. In thermal and chemical problems of thermal waters. *Int. Assoc. Hydrogeol. Sci.* **119**, 17–33.
- Poreda R. J., Craig H., Arnórsson S. & Welhan J. A. (1992) Helium isotopes in Icelandic geothermal systems: I. ^3He , gas chemistry, and ^{13}C relations. *Geochim. Cosmochim. Acta* **56**(12), 4221–4228.
- Poreda R., Schilling J.-G. & Craig H. (1986) Helium and hydrogen isotopes in ocean-ridge basalts north and south of Iceland. *Earth Planet. Sci. Lett.* **78**(1), 1–17.
- Sano Y., Urabe A., Wakita H., Chiba H. & Sakai H. (1985) Chemical and isotopic compositions of gases in geothermal fluids in Iceland. *Geochem. J.* **19**(3), 135–148.
- Torgersen T. & Jenkins W. J. (1982) Helium isotopes in geothermal systems: Iceland, The Geysers, Raft River and Steamboat Springs. *Geochim. Cosmochim. Acta* **46**(5), 739–748.
- Trieloff M., Kunz J., Clague D. A., Harrison D. & Allégre C. J. (2000) The nature of pristine noble gases in mantle plumes. *Science* **288**(5468), 1036–1038.
- Tryggvason K., Husebye E. S. & Stefánsson R. (1983) Seismic image of the hypothesized Icelandic hot spot. *Tectonophysics* **100**, 97–118
- White W. M. (2013). *Geochemistry*. West Sussex: Wiley-Blackwell.
- Winter J. D. (2014) *Principles of Igneous and Metamorphic Petrology* (2nd edition). Essex: Pearson.
- Wolfe C. J., Bjarnason I. Þ., VanDecar J. C. & Solomon S. C. (1997) Seismic structure of the Iceland mantle plume. *Nature* **385**, 245–247

Appendix

The data base used for analysis. The phase is designated with Gf = geothermal fluid, Gl = glass, Ph = phenocryst and Br = breccia.

Sample	Phase	Location	Latitude	Longitude	R _m /R _A	X	R _c /R _A	[He] ^a	Reference
	Gf		65.5118	-23.3822	7.6				Kononov & Polak (1975)
	Gf		65.5756	-23.1230	6.2				Kononov & Polak (1975)
	Gf		65.4522	-22.1695	17.4				Kononov & Polak (1975)
	Gf		65.9100	-22.4489	8.7				Kononov & Polak (1975)
	Gf		65.4650	-20.9424	18.1				Kononov & Polak (1975)
	Gf		65.5449	-20.2055	10.9				Kononov & Polak (1975)
	Gf		65.8741	-19.7545	16.7				Kononov & Polak (1975)
	Gf		65.4785	-19.3690	15.9				Kononov & Polak (1975)
	Gf		66.0221	-18.7613	13.8				Kononov & Polak (1975)
	Gf		65.5727	-17.7375	6.7				Kononov & Polak (1975)
	Gf		65.8965	-17.2779	12.3				Kononov & Polak (1975)
	Gf		65.8000	-16.9666	9.8				Kononov & Polak (1975)
	Gf		65.7059	-16.7528	9.1				Kononov & Polak (1975)
	Gf		65.6051	-16.8412	10.1				Kononov & Polak (1975)
	Gf		66.1311	-16.5099	9.8				Kononov & Polak (1975)
	Gf		65.7929	-14.8819	6.0				Kononov & Polak (1975)
	Gf		64.3249	-15.1954	9.4				Kononov & Polak (1975)
	Gf		64.9843	-15.7871	8.3				Kononov & Polak (1975)
	Gf		65.0678	-15.6708	5.1				Kononov & Polak (1975)
	Gf		65.0425	-16.7094	10.1				Kononov & Polak (1975)
	Gf		64.6593	-17.7895	20.3				Kononov & Polak (1975)

Continued

Sample	Phase	Location	Latitude	Longitude	R_m/R_A	X	R_c/R_A	[He] ^a	Reference
	Gf		64.1567	-19.8006	23.2				Kononov & Polak (1975)
	Gf		64.6781	-19.3291	13.0				Kononov & Polak (1975)
	Gf		63.9952	-19.0447	19.9				Kononov & Polak (1975)
	Gf		63.9415	-19.9470	21.7				Kononov & Polak (1975)
	Gf		64.3284	-20.1967	18.1				Kononov & Polak (1975)
	Gf		64.5810	-20.6327	12.0				Kononov & Polak (1975)
	Gf		64.1367	-20.2882	15.9				Kononov & Polak (1975)
	Gf		64.0419	-21.3565	15.8				Kononov & Polak (1975)
	Gf		64.1381	-21.1650	13.0				Kononov & Polak (1975)
	Gf		64.4382	-21.8710	16.7				Kononov & Polak (1975)
	Gf		64.5224	-21.3105	15.9				Kononov & Polak (1975)
	Gf		64.6889	-21.1375	12.0				Kononov & Polak (1975)
	Gf		63.8398	-22.6242	12.7				Kononov & Polak (1975)
	Gf		65.2528	-21.0558	17.8				Kononov & Polak (1975)
	Gf		64.8637	-19.5161	15.2				Kononov & Polak (1975)
	Gf		64.6780	-19.3183	13.0				Kononov & Polak (1975)
	Gf		65.0255	-18.3100	7.2				Kononov & Polak (1975)
	Gf		65.2925	-19.0605	19.6				Kononov & Polak (1975)
	Gf		65.2745	-18.1805	8.0				Kononov & Polak (1975)
	Gf		64.9058	-23.5836	10.1				Kononov & Polak (1975)
	Gf		64.8378	-23.2467	9.1				Kononov & Polak (1975)
	Gf		64.8280	-22.9380	9.4				Kononov & Polak (1975)
	Gf		64.8278	-22.3056	13.4				Kononov & Polak (1975)
	Gf		64.4807	-21.1490	18.8				Kononov & Polak (1975)
	Gf		64.6558	-21.4225	15.2				Kononov & Polak (1975)
	Gf	Hveravík	65.6833	-21.5500	23.8				Polak et al. (1976)
	Gf	Furubrekka	64.8390	-22.9626	9.03				Polak et al. (1976)
	Gf	Lýsuhóll	64.8402	-23.2245	9.39				Polak et al. (1976)

Continued

Sample	Phase	Location	Latitude	Longitude	R_m/R_A	X	R_c/R_A	[He] ^a	Reference
	Gf	Hveravellir, Kjölur	64.8627	-19.5535	15.2				Polak et al. (1976)
	Gf	Great Geysir	64.3139	-20.3022	19.1				Polak et al. (1976)
	Gf	Hveravellir, Reykjahverfi	65.8864	-17.3096	12.3				Polak et al. (1976)
	Gf	Árhver	64.6500	-21.3500	17.0				Polak et al. (1976)
	Gf	Kerlingarfjöll	64.6237	-19.2958	1.45				Polak et al. (1976)
	Gf	Kerlingarfjöll	64.6237	-19.2958	13.0				Polak et al. (1976)
	Gf	Landmannalaugar	63.9837	-19.0672	18.0				Polak et al. (1976)
	Gf	Hlemmiskeið	64.0167	-20.5500	18.9			1040	Hauksson & Goddard (1981)
	Gf	Selfoss	63.9462	-20.9606	18.3			1380	Hauksson & Goddard (1981)
	Gf	Flúðir	64.1333	-19.9000	17.4			1720	Hauksson & Goddard (1981)
	Gf	Flúðir	64.1333	-19.9000	17.6			1740	Hauksson & Goddard (1981)
G-31	Gf	Reykjavík	64.1500	-21.9333	11.6			201	Torgersen & Jenkins (1982)
	Gf	Reykjavík	64.1500	-21.9333	10.7			201	Torgersen & Jenkins (1982)
G-10	Gf	Reykjavík	64.1500	-21.9333	12.7			172	Torgersen & Jenkins (1982)
KJ-7	Gf	Krafla	65.7167	-16.7333	8.4			23570	Torgersen & Jenkins (1982)
KG-8	Gf	Krafla	65.7167	-16.7333	7.9			11740	Torgersen & Jenkins (1982)
	Gf	Krafla	65.7167	-16.7333	9.0			4160	Torgersen & Jenkins (1982)
	Gf	Krafla	65.7167	-16.7333	8.3			1070	Torgersen & Jenkins (1982)
	Gf	Hafralækur	65.8667	-17.4333	9.0			203	Torgersen & Jenkins (1982)
138413	Gl	Stapafell, south part	63.9000	-22.5167	23.9			52	Condomines et al. (1983)
115619	Gl	Stapafell, west part	63.9000	-22.5167	13.8			52.1	Condomines et al. (1983)
RP	Gl	Reykjanes	63.8000	-22.6833	13.7			640	Condomines et al. (1983)
Krísuvík	Gl	Reykjanes peninsula	63.8333	-22.2833	13.4			33.8	Condomines et al. (1983)
HEN 1	Gl	Hengill	64.0167	-21.3833	12.4			101	Condomines et al. (1983)
TOR103	Gl	Þórisjökull	64.5333	-20.7000	12.3			106	Condomines et al. (1983)
TOR108	Gl	Þórisjökull	64.5333	-20.7000	12.7			27	Condomines et al. (1983)
138359	Gl	Hrauneyjarfoss	64.2000	-19.2333	21.3			136	Condomines et al. (1983)
A2	Gl	Askja	65.0333	-16.7167	7.1			42.6	Condomines et al. (1983)

Continued

Sample	Phase	Location	Latitude	Longitude	R_m/R_A	R_c/R_A	[He] ^a	Reference
NAL 33	Gl	Hvammssfjöll	65.3500	-16.6667	10.1		404	Condomines et al. (1983)
NAL 34	Gl	Eggert	65.2500	-16.4667	9.8		55.2	Condomines et al. (1983)
KRA 81	Gl	Krafla	65.7167	-16.7833	5.07		42.3	Condomines et al. (1983)
Tephra	Gl	Grímsvötn	64.4167	-17.3333	3.59		129	Condomines et al. (1983)
KER 226	Gl	Kerlingarfjöll	64.6333	-19.2833	1.5		300	Condomines et al. (1983)
H 70-16	Gl	Hekla	63.9833	-19.6667	1.02		12.5	Condomines et al. (1983)
SAL 74	Gl	Öræfajökull	64.0333	-16.6500	1.14		18	Condomines et al. (1983)
A1875	Gl	Askja	65.0333	-16.7167	0.93		60	Condomines et al. (1983)
KK 26	Gl	Krafla	65.7167	-16.7833	1.06		34	Condomines et al. (1983)
ATHO	Gl	Krafla	65.7167	-16.7833	0.82		10	Condomines et al. (1983)
87841	Gl	Þingmúli	65.0167	-14.6500	0.072		73	Condomines et al. (1983)
EZ-274	Ph	Stapafell	63.9000	-22.5300	13.9		9.3	Kurz et al. (1985)
VM-10	Ph	Heimaey	63.4000	-20.2800	11.0		12	Kurz et al. (1985)
EZ-274	Gl	Stapafell	63.9000	-22.5300	14.0		11	Kurz et al. (1985)
SK82-29C	Gl	Stapafell	63.9000	-22.5300	13.9		151.3	Kurz et al. (1985)
SK82-12	Br	Kálfstindar	64.2400	-20.7400	13.8		1430	Kurz et al. (1985)
SK82-28	Gl	Kálfstindar	64.2400	-20.7400	14.2		1630	Kurz et al. (1985)
HS-785	Gl	Botnsheiði	64.4500	-21.0800	15.2		30	Kurz et al. (1985)
SK82-01B	Gl	Vestur Jarlhettur	64.4600	-20.2500	15.9		62	Kurz et al. (1985)
HS-806	Gl	Eiríksjökull	64.8000	-20.4500	8.67		154	Kurz et al. (1985)
IC-117	Gl	Dvergalda	65.0000	-19.5800	21.6		1360	Kurz et al. (1985)
SK82-05	Gl	SW of Blágnípa	64.7300	-19.1800	20.9		143	Kurz et al. (1985)
SK82-06	Gl	SW of Blágnípa	64.7300	-19.1800	20.0		1110	Kurz et al. (1985)
EZ 125B	Gl	Innsta-Bálkafell	64.6800	-17.6800	22.2		62	Kurz et al. (1985)
EZ 120	Gl	Tindafell	64.7300	-17.6500	19.7		39.2	Kurz et al. (1985)
EZ-179	Gl	Heljargjá	64.3200	-18.4600	20.0		302	Kurz et al. (1985)
EZ-149B	Gl	Grasatangi	64.2300	-18.9900	18.0		13	Kurz et al. (1985)
SK82-27	Gl	Sigalda	64.1500	-19.1300	20.8		175	Kurz et al. (1985)

Continued

Sample	Phase	Location	Latitude	Longitude	R _m /R _A	X	R _c /R _A	[He] ^a	Reference
EZ-210	Gl	Faxasund	64.0300	-18.6900	20.7			1240	Kurz et al. (1985)
HE-35	Gl	Sauðleysur	64.0700	-19.3500	20.2			23.5	Kurz et al. (1985)
HE-24	Gl	Stóraskógsbotnar	63.9600	-19.8600	13.9			19	Kurz et al. (1985)
SK82-13	Gl	Þríhyrningur	63.7800	-19.9500	26.2			455	Kurz et al. (1985)
IC-152	Gl	Krafla	65.6200	-17.0800	11.0			152	Kurz et al. (1985)
	Gf	Krafla	65.7167	-16.7333	9.1	86.75	9.2	20.9	Sano et al. (1985)
	Gf	Krafla	65.7167	-16.7333	8.6	73.73	8.7	135	Sano et al. (1985)
	Gf	Hveragerði	64.0000	-21.1833	8.1	477	8.1	36	Sano et al. (1985)
	Gf	Námafjall	65.6333	-16.8167	8.7	156	8.7	<100	Sano et al. (1985)
	Gf	Víðigerði	64.6667	-21.4000	8.4	16.48	8.9		Sano et al. (1985)
	Gf	Geysir	64.3167	-20.3000	12.0	17.35	12.7		Sano et al. (1985)
	Gf	Geysir	64.3167	-20.3000	17.0	25.59	17.7	121	Sano et al. (1985)
	Gf	Laugarvatn	64.2000	-20.7000	2.1	3.43	2.6		Sano et al. (1985)
	Gf	Reykjanes	63.8167	-22.7000	3.5	2.13	5.7	9	Sano et al. (1985)
	Gf	Reykjanes	63.8167	-22.7000	3.7	3.04	5		Sano et al. (1985)
	Gf	Krísuvík	63.9000	-22.0500	13.7	130	13.8	11	Sano et al. (1985)
	Gl	Stakksá	64.2667	-20.2833	16.5	100	16.7	5.9	Poreda et al. (1986)
	Gl	Kálfstindar	64.2500	-20.8667	13.9	1000	13.9	380	Poreda et al. (1986)
	Gl	Surtsey	63.3000	-20.5833	13.6	150	13.7	4.8	Poreda et al. (1986)
RE-78	Ph	Vatnsheiði	63.8667	-22.3833	12.5	20	13.1	1.4	Poreda et al. (1986)
	Ph	Miðfell	64.1833	-21.0000	16.1	40	16.5	2.6	Poreda et al. (1986)
	Ph	Surtsey	63.3000	-20.5833	15.1	50	15.3	22	Poreda et al. (1986)
	Ph	Hvammsmúli	63.5740	-19.8700	12.2			0.2	Poreda et al. (1986)
R-Nes-N	Gf	Reykjanes	63.8167	-22.6833	11.0	10.6	12		Hilton et al. (1990)
R-Nes-M	Gf	Reykjanes	63.8167	-22.6833	9.9	20.9	10.3		Hilton et al. (1990)
R-Nes-S	Gf	Reykjanes	63.8167	-22.6833	13.9	31.8	14.4		Hilton et al. (1990)
8	Gf	Reykjanes	63.8167	-22.6833	12.2	275.8	12.2		Hilton et al. (1990)
6	Gf	Svartsengi	63.8833	-22.4333	13.4	83.8	13.5		Hilton et al. (1990)

Continued

Sample	Phase	Location	Latitude	Longitude	R_m/R_A	X	R_c/R_A	[He] ^a	Reference
6	Gf	Svartsengi	63.8833	-22.4333	13.6	30.1	14	360	Hilton et al. (1990)
8	Gf	Svartsengi	63.8833	-22.4333	13.1	65.8	13.3		Hilton et al. (1990)
9	Gf	Svartsengi	63.8833	-22.4333	12.4	140.6	12.5		Hilton et al. (1990)
9	Gf	Svartsengi	63.8833	-22.4333	14.2	137.6	14.3	280	Hilton et al. (1990)
10	Gf	Svartsengi	63.8833	-22.4333	13.0	15	13.9		Hilton et al. (1990)
11	Gf	Svartsengi	63.8833	-22.4333	11.6	34	11.9		Hilton et al. (1990)
11	Gf	Hengill	64.1000	-21.2667	15.2	6.2	17.9		Hilton et al. (1990)
Geysir	Gf	Geysir	64.3167	-20.3000	14.7	8.5	16.5	140	Hilton et al. (1990)
Great Geysir	Gf	Geysir	64.3167	-20.3000	15.7	8.3	17.7	310	Hilton et al. (1990)
3110	Gf	Torfajökull	63.9000	-19.0667	9.8	4	12.8		Hilton et al. (1990)
Skeiðará	Gf	Grímsvötn	64.4123	-17.3326	17.3	18.7	18.2	1000	Hilton et al. (1990)
Skeiðará	Gf	Grímsvötn	64.4123	-17.3326	15.3	4	19	400	Hilton et al. (1990)
BJ-3153	Gf	Námafjall	65.6333	-16.8167	8.0	5.1	9.7		Hilton et al. (1990)
BJ-12	Gf	Námafjall	65.6333	-16.8167	8.4				Hilton et al. (1990)
KG-8	Gf	Krafla	65.7167	-16.7667	8.6	82.2	8.7		Hilton et al. (1990)
KJ-15	Gf	Krafla	65.7167	-16.7667	9.4				Hilton et al. (1990)
KJ-16	Gf	Krafla	65.7167	-16.7667	9.4				Hilton et al. (1990)
Víti	Gf	Krafla	65.7167	-16.7500	8.4				Hilton et al. (1990)
Leirhnjúkur	Gf	Krafla	65.7167	-16.8167	8.6				Hilton et al. (1990)
Hveragil	Gf	Krafla	65.7167	-16.7667	8.7	66.8	8.8	820	Hilton et al. (1990)
G-1	Gf	Þeistareykir	65.8833	-16.9500	8.9	27	9.2		Hilton et al. (1990)
G-7	Gf	Þeistareykir	65.8833	-16.9500	6.9				Hilton et al. (1990)
	Gf	Eyvík	64.0333	-20.7000	21.4	83.2	21.7	3080	Hilton et al. (1990)
	Gf	Herríðarhóll	63.9333	-20.5500	14.6	13.9	15.7	750	Hilton et al. (1990)
	Gf	Hjallanes	63.9667	-20.4333	14.3	6.2	16.9	410	Hilton et al. (1990)
	Gf	Hlemmiskeið	64.0167	-20.5667	17.9	54.9	18.2	1310	Hilton et al. (1990)
	Gf	Laugaland	63.9167	-20.4000	19.7	54.7	20	630	Hilton et al. (1990)
	Gf	Ormsstaðir	64.0333	-20.7000	21.1	22.2	22	8430	Hilton et al. (1990)

Continued

Sample	Phase	Location	Latitude	Longitude	R_m/R_A	X	R_c/R_A	[He] ^a	Reference
	Gf	Þjórsárdalur	64.1000	-19.9000	20.7	55.7	21.1	1520	Hilton et al. (1990)
	Gf	Þjórsárholt	64.0167	-20.2667	17.8	16.1	18.9	3350	Hilton et al. (1990)
	Gf	Þorleifskot	63.9500	-20.6000	17.8	30.9	18.4	920	Hilton et al. (1990)
	Gf	Þóróddsstaðir	63.9667	-21.3000	17.0	51	17.4	2660	Hilton et al. (1990)
	Gf	Þorlákshver	64.1000	-20.6000	13.3	14.2	14.2	320	Hilton et al. (1990)
	Gf	Reykir Skeið	64.0500	-20.6000	13.2	34.2	13.5	900	Hilton et al. (1990)
	Gf	Skarð	64.0000	-20.1000	16.6	4.7	20.8	610	Hilton et al. (1990)
	Gf	Sólheimar	64.0667	-20.6500	18.8	27.8	19.5	700	Hilton et al. (1990)
	Gf	Spóastaðir	64.1333	-20.6500	17.8	26.3	18.5	2130	Hilton et al. (1990)
	Gf	Vatnsnes	64.0167	-20.6500	20.1	12.4	21.8	180	Hilton et al. (1990)
	Gf	Borðeyri	65.2167	-21.1167	17.4	257.7	17.4	32600	Hilton et al. (1990)
	Gf	Gjögur	65.9833	-21.3500	13.4	12.3	14.5	620	Hilton et al. (1990)
	Gf	Hveravík	65.7000	-21.5667	25.4	33.2	26.2	580	Hilton et al. (1990)
	Gf	Laugarhóll	65.7833	-21.5167	4.1	2.5	6.1	320	Hilton et al. (1990)
MG-5	Gf	Mosfellssveit	64.1667	-21.7000	13.1	12.3	14.1	520	Hilton et al. (1990)
MG-5	Gf	Mosfellssveit	64.1667	-21.7000	12.8	10.8	14	490	Hilton et al. (1990)
MG-16	Gf	Mosfellssveit	64.1667	-21.7000	13.7	19.3	14.4	1180	Hilton et al. (1990)
MG-17	Gf	Mosfellssveit	64.1667	-21.7000	12.6	8.8	14.1	370	Hilton et al. (1990)
MG-18	Gf	Mosfellssveit	64.1667	-21.7000	12.0	6.3	14.1	330	Hilton et al. (1990)
MG-35	Gf	Mosfellssveit	64.1667	-21.7000	13.5	24	14	1020	Hilton et al. (1990)
MG-37	Gf	Mosfellssveit	64.1667	-21.7000	13.9	27.6	14.4	90	Hilton et al. (1990)
G-5	Gf	Reykjavík	64.1500	-21.9333	11.0	6.7	12.7	340	Hilton et al. (1990)
G-35	Gf	Reykjavík	64.1500	-21.9333	11.2	6.9	13	480	Hilton et al. (1990)
G-37	Gf	Reykjavík	64.1500	-21.9333	9.7	4.4	12.3	260	Hilton et al. (1990)
RG-30	Gf	Reykjavík	64.1500	-21.9333	11.0	5.3	13.3	330	Hilton et al. (1990)
RG-31	Gf	Reykjavík	64.1500	-21.9333	9.8	3.9	12.8	900	Hilton et al. (1990)
SN-4	Gf	Seltjarnarnes	64.1500	-21.9833	12.7	10.4	14	1060	Hilton et al. (1990)
SN-4	Gf	Seltjarnarnes	64.1500	-21.9833	12.0	11.1	13.1	530	Hilton et al. (1990)

Continued

Sample	Phase	Location	Latitude	Longitude	R_m/R_A	X	R_c/R_A	[He] ^a	Reference
SN-5	Gf	Seltjarnarnes	64.1500	-21.9833	12.2	8.4	13.7	580	Hilton et al. (1990)
	Gf	Hafragil	65.8333	-19.9000	10.1	16.4	10.7	890	Hilton et al. (1990)
	Gf	Laugaland	65.7500	-18.2500	8.4	15.9	8.9	370	Hilton et al. (1990)
NG09	Gf	Nesjavellir	64.1167	-21.2500	14.8			4.62	Marty et al. (1991)
NJ11	Gf	Nesjavellir	64.1167	-21.2500	14.5			0.79	Marty et al. (1991)
NJ13	Gf	Nesjavellir	64.1167	-21.2500	14.6			1.59	Marty et al. (1991)
NES1	Gf	Nesjavellir	64.1167	-21.2500	14.7			3.05	Marty et al. (1991)
NES2	Gf	Nesjavellir	64.1167	-21.2500	14.1			14.62	Marty et al. (1991)
NES3	Gf	Nesjavellir	64.1167	-21.2500	14.7			3.39	Marty et al. (1991)
NES4	Gf	Nesjavellir	64.1167	-21.2500	12.4			3.90	Marty et al. (1991)
NES5	Gf	Nesjavellir	64.1167	-21.2500	14.6			1.71	Marty et al. (1991)
NES6	Gf	Nesjavellir	64.1167	-21.2500	11.9			2.00	Marty et al. (1991)
HEL1	Gf	South Hengill	64.0833	-21.3167	13.1			4.65	Marty et al. (1991)
HEL4	Gf	South Hengill	64.0833	-21.3167	13.6			1.21	Marty et al. (1991)
HEL7	Gf	South Hengill	64.0833	-21.3167	14.3			2.55	Marty et al. (1991)
HEL2	Gf	South Hengill	64.0833	-21.3167	14.6			1.25	Marty et al. (1991)
HEL3	Gf	South Hengill	64.0833	-21.3167	14.7			0.35	Marty et al. (1991)
HEL5	Gf	South Hengill	64.0833	-21.3167	14.1			0.39	Marty et al. (1991)
HEL6	Gf	South Hengill	64.0833	-21.3167	13.6			1.26	Marty et al. (1991)
HVG1	Gf	Hveragerði	64.0000	-21.1833	14.9			0.68	Marty et al. (1991)
HVG2	Gf	Hveragerði	64.0000	-21.1833	14.8			0.68	Marty et al. (1991)
79-1	Gf	Flúðir	64.1333	-20.3167	17.4	30	18	96.9	Poreda et al. (1992)
79-2	Gf	Hlemmiskeið	64.0167	-20.5500	18.9	26	19.5	76.7	Poreda et al. (1992)
79-3	Gf	Syðra Langholt	64.0833	-20.4333	18.2	25.7	18.8	73.8	Poreda et al. (1992)
79-4	Gf	Selfoss	63.9333	-21.0000	18.3	40	18.7		Poreda et al. (1992)
I81-6	Gf	Geysir	64.3167	-20.3000	11.41	5.3	13.6	13.2	Poreda et al. (1992)
I83-118	Gf	Geysir	64.3167	-20.3000	18.56	95	18.73	49.2	Poreda et al. (1992)
I81-7	Gf	Reykholt	64.1749	-20.4482	17.82			175	Poreda et al. (1992)

Continued

Sample	Phase	Location	Latitude	Longitude	R_m/R_A	X	R_c/R_A	[He] ^a	Reference
I81-8	Gf	Flúðir	64.1333	-19.9000	18.72	29	19.23	43.1	Poreda et al. (1992)
I81-10	Gf	Seltjarnares	64.1500	-21.9833	15.4	34	15.76	27.0	Poreda et al. (1992)
I81-17	Gf	Reykir	64.1667	-21.6667	14.23	39	14.54	23.6	Poreda et al. (1992)
I81-18	Gf	Reykir	64.1667	-21.6667	14.62	19.2	15.23	72.5	Poreda et al. (1992)
I81-19	Gf	Reykjanes	63.8167	-22.6833	14.3	39	14.62	7.89	Poreda et al. (1992)
I81-20	Gf	Reykjanes	63.8167	-22.6833	14.38	286	14.42	5.87	Poreda et al. (1992)
I81-21	Gf	Svartsengi	63.8833	-22.4333	13.68	10.5	15	12.0	Poreda et al. (1992)
I81-22	Gf	Hveragerði	64.0000	-21.1833	17.69	39	18.09	7.80	Poreda et al. (1992)
I83-119	Gf	Nesjavellir	64.1167	-21.2500	15.8	215	15.86	13.2	Poreda et al. (1992)
I83-124	Gf	Klausturhólar	64.0667	-20.8333	19.07	33	19.53	6.00	Poreda et al. (1992)
84-3105	Gf	Krísuvík	63.8833	-22.0500	14.46	175	14.53	8.38	Poreda et al. (1992)
I83-101	Gf	Árhver	64.6500	-21.3500	15.61	55	15.85	72.6	Poreda et al. (1992)
I83-102	Gf	Lýsuhóll	64.8333	-23.2167	9.32			251	Poreda et al. (1992)
I83-104	Gf	Rauðamelsölkelda	64.9000	-22.3333	12.25	1000	12.25	34.8	Poreda et al. (1992)
I83-107	Gf	Sælingsdalur	65.2667	-21.8333	12.73	14	13.6		Poreda et al. (1992)
I83-106	Gf	Reykhólar	65.4500	-22.2000	16.93	34	17.4	101	Poreda et al. (1992)
I83-108	Gf	Borðeyri	65.2000	-21.1000	17.27	1300	17.28	2002	Poreda et al. (1992)
I85	Gf	Svannshóll	65.7833	-21.5333	11.2	4.3	14.2	10.10	Poreda et al. (1992)
I85	Gf	Krossnes	66.0000	-21.5167	27.3	15.8	28.8	7.40	Poreda et al. (1992)
I85	Gf	Hveravík	65.7000	-21.5667	25.8	60	26.2	154	Poreda et al. (1992)
I83-116	Gf	Hveravellir	64.8667	-19.5500	16.26	100	16.4	18.2	Poreda et al. (1992)
I83-117	Gf	Kerlingarfjöll	64.6333	-19.3000	16.56	120	16.68	6.42	Poreda et al. (1992)
I81-9	Gf	Þjórsárdalur	64.1000	-19.9000	22.87	50	23.27	315	Poreda et al. (1992)
I81-33	Gf	Landmannalaugar	63.9833	-19.0667	22.57	55	22.93	20.0	Poreda et al. (1992)
I83-120	Gf	Landmannalaugar	63.9833	-19.0667	18.91	5	23.4	2.22	Poreda et al. (1992)
I83-123	Gf	Landmannalaugar	63.9833	-19.0667	23.14	38	23.74	2.18	Poreda et al. (1992)
85-3092	Gf	Köldukvíslarbotnar	64.6000	-17.9333	25.77	125	25.95	36.0	Poreda et al. (1992)
85-3014	Gf	Vonarskarð	64.5833	-18.0167	20.5	54	20.87	2.57	Poreda et al. (1992)

Continued

Sample	Phase	Location	Latitude	Longitude	R_m/R_A	X	R_c/R_A	[He] ^a	Reference
I83-110	Gf	Askja	65.0500	-16.8000	10.37	100	10.45	6.47	Poreda et al. (1992)
I83-111	Gf	Kverkfjöll	64.6500	-16.7167	8.47	100	8.54	5.80	Poreda et al. (1992)
I83-112	Gf	Kverkfjöll	64.6500	-16.7167	8.81	220	8.84	8.02	Poreda et al. (1992)
I83-114	Gf	Námafjall	65.6333	-16.8167	9.24	34	9.46	3.78	Poreda et al. (1992)
I83-115	Gf	Námafjall	65.6333	-16.8167	9.77	57	9.91	14.2	Poreda et al. (1992)
85-3020	Gf	Námafjall	65.6333	-16.8000	8.8	9.8	9.68	3.97	Poreda et al. (1992)
I83-113	Gf	Krafla, Víti	65.7167	-16.7500	9.74	4000	9.74	21.4	Poreda et al. (1992)
85-3015	Gf	Krafla	65.7000	-16.7333	9.44	320	9.46	10.7	Poreda et al. (1992)
85-3016	Gf	Krafla	65.7000	-16.7333	9.41	840	9.42	15.3	Poreda et al. (1992)
85-3017	Gf	Krafla	65.7000	-16.7333	9.48	1000	9.49	39.0	Poreda et al. (1992)
85-3019	Gf	Krafla, Leirhnúkur	65.7000	-16.8167	9.36	200	9.4	21.4	Poreda et al. (1992)
I85	Gf	Ærlækjarsel	66.1500	-16.5333	10.05	40	10.28	175	Poreda et al. (1992)
85-3018	Gf	Þeistareykir	65.8833	-16.9500	10.6	140	10.66	19.1	Poreda et al. (1992)
85-3088	Gf	Þveit	64.3500	-15.2667	9.73	250	9.76	7.97	Poreda et al. (1992)
85-3089	Gf	Bæjarstaðaskógur	64.0667	-17.0167	13.57	57	13.76	66.5	Poreda et al. (1992)
85-3086	Gf	Seljavallalaug	63.5667	-19.6000	17.98	11.2	19.2	5.83	Poreda et al. (1992)
80	Gf	Lagarfljót	64.9167	-15.0833	2.7	1.6	5	0.34	Poreda et al. (1992)
MIDgl cr2	Gl	Miðfell	64.1667	-21.0333	16.8			0.00089	Burnard et al. (1994)
HENglb cr1	Gl	Hengill	64.0167	-21.3833	16.8			0.0005	Burnard et al. (1994)
HENglb cr2	Gl	Hengill	64.0167	-21.3833	16.8			0.00018	Burnard et al. (1994)
HENglb cr3	Gl	Hengill	64.0167	-21.3833	16.8			0.000033	Burnard et al. (1994)
NAL216 cr2	Gl	Hvammfjöll	65.3500	-16.6667	12.3			0.00009	Burnard et al. (1994)
NAL281 cr4	Gl	Herðubreiðarfjöll	65.3667	-16.3667	12.8			0.00006	Burnard et al. (1994)
MIDol cr2	Ph	Miðfell	64.1667	-21.0333	13.7			0.000009	Burnard et al. (1994)
HENol cr2	Ph	Hengill	64.0167	-21.3833	16.8			0.000006	Burnard et al. (1994)
	Gf	Djúpidalur	65.5833	-22.2833	23.6	13.7	24.9	1580	Hilton et al. (1998)
	Gf	Djúpidalur	65.5833	-22.2833	24.2	12.7	25.7	996	Hilton et al. (1998)
	Gf	Flókalundur	65.5833	-23.1667	6.23	2.61	8.36	185	Hilton et al. (1998)

Continued

Sample	Phase	Location	Latitude	Longitude	R _m /R _A	X	R _c /R _A	[He] ^a	Reference
	Gf	Goðdalur	65.8167	-21.5833	3.42	1.06	9.48		Hilton et al. (1998)
	Gf	Goðdalur	65.8167	-21.5833	2.81	1.15	6.28	29	Hilton et al. (1998)
	Gf	Gjögur	66.0000	-21.3333	15.8	24.4	16.3		Hilton et al. (1998)
	Gf	Gjögur	66.0000	-21.3333	14.8	20.7	15.3	473	Hilton et al. (1998)
	Gf	Hörgshlíð	65.8500	-22.6167	16.9	3.45	21.3	119	Hilton et al. (1998)
	Gf	Hörgshlíð	65.8500	-22.6167	16.6	5.32	19.2	203	Hilton et al. (1998)
	Gf	Hveratunga	65.8667	-21.3667	4.21	1.62	7.02	28.1	Hilton et al. (1998)
	Gf	Hveratunga	65.8667	-21.3667	4.31	1.53	7.56	26	Hilton et al. (1998)
	Gf	Hveravík	65.7000	-21.5667	22.3	44.2	22.7	1206	Hilton et al. (1998)
	Gf	Hveravík	65.7000	-21.5667	23.0	40.5	23.4	1113	Hilton et al. (1998)
	Gf	Kirkjuból	66.2500	-22.1000	8.85	17.7	9.17		Hilton et al. (1998)
	Gf	Kirkjuból	66.2500	-22.1000	8.63	18	8.97	655	Hilton et al. (1998)
	Gf	Kirkjuból	66.2500	-22.1000	8.6	17.7	8.94	480	Hilton et al. (1998)
	Gf	Krossholt	65.4833	-23.2667	9.22	4.62	10.8	482	Hilton et al. (1998)
	Gf	Krossnes	66.0500	-21.5000	24.1	42.6	24.5		Hilton et al. (1998)
	Gf	Krossnes	66.0500	-21.5000	23.9	3.43	30.4	918	Hilton et al. (1998)
	Gf	Krossnes	66.0500	-21.5000	25.3	13.1	26.8		Hilton et al. (1998)
	Gf	Krossnes	66.0500	-21.5000	24.2	7.98	26.6	504	Hilton et al. (1998)
	Gf	Krossnes	66.0500	-21.5000	25.2	7.82	27.8	518	Hilton et al. (1998)
	Gf	Laugaland	66.0167	-22.3833	3.4	4.06	3.95		Hilton et al. (1998)
	Gf	Laugaland	66.0167	-22.3833	3.34	3.98	3.89		Hilton et al. (1998)
	Gf	Laugaland	66.0167	-22.3833	2.9	2.51	3.72	181	Hilton et al. (1998)
	Gf	Laugarhóll	65.7833	-21.5167	8.44	1.95	13.2		Hilton et al. (1998)
	Gf	Laugardalsá	65.6500	-23.9000	12.5	1.71	21.6	73.8	Hilton et al. (1998)
	Gf	Laugardalsá	65.6500	-23.9000	15.2	2.39	21.8	134	Hilton et al. (1998)
	Gf	Reykhólar	65.4500	-22.2167	15.2	22.3	15.7		Hilton et al. (1998)
	Gf	Reykhólar	65.4500	-22.2167	16.9	21.4	17.4		Hilton et al. (1998)
	Gf	Reykjanes	65.9333	-22.4333	2.08	1.48	3.21	37.9	Hilton et al. (1998)

Continued

Sample	Phase	Location	Latitude	Longitude	R_m/R_A	X	R_c/R_A	[He] ^a	Reference
	Gf	Reykjanes	65.9333	-22.4333	2.36	2.09	3.14	36.3	Hilton et al. (1998)
	Gf	Reykjafjörður	65.6167	-23.4667	3.82	1.14	9.36		Hilton et al. (1998)
	Gf	Reykjafjörður	65.6167	-23.4667	4.29	1.5	7.66	35.9	Hilton et al. (1998)
Dice 11	Gl	Dagmálafell	64.1769	-21.0503	16.59			5630	Harrison et al. (1999)
Dice 10	Gl	Dagmálafell	64.1769	-21.0503	17.46			1290	Harrison et al. (1999)
SE13	Ph	Selárdalur	65.7667	-24.0000	37.3			1.21	Hilton et al. (1999)
SE-21	Ph	Selárdalur	65.7667	-24.0000	18.8			0.6	Hilton et al. (1999)
3951	Ph	Selárdalur	65.7667	-24.0000	37.7			0.89	Hilton et al. (1999)
3951	Ph	Selárdalur	65.7667	-24.0000	30.1			1.2	Hilton et al. (1999)
SEL97	Ph	Selárdalur	65.7667	-24.0000	35.7			0.37	Hilton et al. (1999)
SEL97	Ph	Selárdalur	65.7667	-24.0000	37.5			6.5	Hilton et al. (1999)
408709	Gl	Kistufell	64.7939	-17.1819	15.65			293	Breddam et al. (2000)
408710	Gl	Kistufell	64.7939	-17.1806	15.79			39.2	Breddam et al. (2000)
408706	Gl	Kistufell	64.7958	-17.1811	15.33			162	Breddam et al. (2000)
408707	Gl	Kistufell	64.7958	-17.1811	15.69			480	Breddam et al. (2000)
408712	Gl	Kistufell	64.8033	-17.2153	16.79			261	Breddam et al. (2000)
408702	Gl	Kambsfell	64.8297	-17.7681	20.37			440	Breddam et al. (2000)
408713	Gl	Dyngjufjöll Ytri	65.1656	-16.9250	19.58			86	Breddam et al. (2000)
408714	Gl	Dyngjufjöll Ytri	65.1658	-16.9308	19.53			85.1	Breddam et al. (2000)
408730	Gl	Bláfjall	65.4903	-16.8519	10.54			281	Breddam et al. (2000)
408729	Gl	Bláfjall	65.4911	-16.8492	10.76			92.7	Breddam et al. (2000)
408732	Gl	Bláfjall	65.5194	-16.8450	13.38			18.66	Breddam et al. (2000)
408718	Gl	Gæsafjöll	65.7544	-16.9258	11.56			13.34	Breddam et al. (2000)
408719	Gl	Gæsafjöll	65.7544	-16.9258	12.34			58.2	Breddam et al. (2000)
408722	Gl	Gæsafjöll	65.7592	-16.9239	11.49			5.72	Breddam et al. (2000)
408723	Gl	Gæsafjöll	65.7592	-16.9239	11.63			31.1	Breddam et al. (2000)
sk82-05	Gl	SW of Blágnípa	64.7300	-19.1800	20.9			143	Breddam et al. (2000)
sk82-06	Gl	SW of Blágnípa	64.7300	-19.1800	20.0			1110	Breddam et al. (2000)

Continued

Sample	Phase	Location	Latitude	Longitude	R_m/R_A	X	R_c/R_A	[He] ^a	Reference
sk82-13	Gl	Þríhyrningur	63.7800	-19.9500	26.2			455	Breddam et al. (2000)
sk82-27	Gl	Sigalda	64.1500	-19.9167	20.8			175	Breddam et al. (2000)
sk82-28	Gl	Kálfstindar	64.2400	-20.7400	14.2			1630	Breddam et al. (2000)
sk82-29	Gl	Stapafell	63.9000	-22.5300	13.9			1430	Breddam et al. (2000)
207901	Ph	Háleyjabunga	63.8167	-22.6333	10.89			0.52	Breddam et al. (2000)
208222	Ph	Vatnsheiði	63.8389	-22.3942	11.65			4.26	Breddam et al. (2000)
408672	Ph	Lagafell	63.8811	-22.5394	14.09			1.53	Breddam et al. (2000)
408634	Ph	Þeistareykir	65.9353	-17.0778	8.16			0.49	Breddam et al. (2000)
408635	Ph	Þeistareykir	65.9369	-17.0800	9.47			2.69	Breddam et al. (2000)
408643	Ph	Þeistareykir	65.9467	-17.1419	8.92			0.3	Breddam et al. (2000)
408640	Ph	Þeistareykir	65.9611	-17.0756	9.75			42.6	Breddam et al. (2000)
408647	Ph	Þeistareykir	65.9625	-16.9039	7.99			2.59	Breddam et al. (2000)
ice-9a	Ph	Búrfell í Ölfusi	64.1833	-21.0667	20.0			8.5	Dixon et al. (2000)
ice-9b	Ph	Búrfell í Ölfusi	64.1833	-21.0667	29.0			9.3	Dixon et al. (2000)
ice-9c	Ph	Búrfell í Ölfusi	64.1833	-21.0667	17.0			7.9	Dixon et al. (2000)
ice-9d	Ph	Búrfell í Ölfusi	64.1833	-21.0667	20.0			11.7	Dixon et al. (2000)
ice-18b	Ph	Stapafell	63.9167	-22.5333	16.0			9.7	Dixon et al. (2000)
ice-19a	Ph	Súlur	63.9000	-22.5333	17.0			11	Dixon et al. (2000)
ice-19b	Ph	Súlur	63.9000	-22.5333	15.0			14.5	Dixon et al. (2000)
ice-30	Ph	Landmannahellir	64.2167	-20.9000	14.2			8.5	Dixon et al. (2000)
ice32.1a	Ph	Svartengisfell	63.8833	-22.4333	15.0			18.7	Dixon et al. (2000)
ice34-a	Ph	Ísólfskáli	63.8608	-22.3178	12.0			3.9	Dixon et al. (2000)
ice-9g1	Gl	Búrfell í Ölfusi	64.1833	-21.0667	17.0			932.7	Dixon et al. (2000)
ice9g2	Gl	Búrfell í Ölfusi	64.1833	-21.0667	19.0			6237.5	Dixon et al. (2000)
ice9g3	Gl	Búrfell í Ölfusi	64.1833	-21.0667	19.0			2377.2	Dixon et al. (2000)
ice-18g2	Gl	Stapafell	63.9167	-22.5333	14.0			52	Dixon et al. (2000)
ice-18g3	Gl	Stapafell	63.9167	-22.5333	14.0			61.9	Dixon et al. (2000)
ice32.2g1	Gl	Svartengisfell	63.8833	-22.4333	13.0			39.1	Dixon et al. (2000)

Continued

Sample	Phase	Location	Latitude	Longitude	R _m /R _A	X	R _c /R _A	[He] ^a	Reference
ice-32.2g2	Gl	Svartengisfell	63.8833	-22.4333	18.0			17.3	Dixon et al. (2000)
ice-47g	Gl	Sigalda	64.1667	-19.1667	20.0			292.8	Dixon et al. (2000)
ice-54g	Gl	Lambafell	64.0167	-21.4667	19.0			21.4	Dixon et al. (2000)
ice-55g	Gl	Kóngsgil	64.0333	-21.4167	20.0			27	Dixon et al. (2000)
Dice 10	Gl	Dagmálafell	64.1769	-21.0503	17.2				Trieloff et al. (2000)
Dice 11	Gl	Dagmálafell	64.1769	-21.0503	17.39				Trieloff et al. (2000)
KBD 408 702	Gl	Kambsfell	64.8297	-17.7681	20.6			430	Moreira et al. (2001)
KBD 408 706	Gl	Kistufell	64.7958	-17.1811	15.5			10000	Moreira et al. (2001)
KBD 408 707	Gl	Kistufell	64.7958	-17.1811	16.1			1200	Moreira et al. (2001)
KBD 408 709	Gl	Kistufell	64.7939	-17.1819	16.0			1600	Moreira et al. (2001)
KBD 408 730	Gl	Bláfjall	65.4903	-16.8519	10.0			290	Moreira et al. (2001)
SK 82-13	Gl	Þríhyrningur	63.7800	-19.9500	25.6			304	Moreira et al. (2001)
SK 82-28	Gl	Kálfstindar	64.2400	-20.7400	14.3			2860	Moreira et al. (2001)
ice-1a	Ph	Miðfell	64.1760	-21.0570	18.0			2.9	Dixon (2003)
ice-1b	Ph	Miðfell	64.1760	-21.0570	21.0			5	Dixon (2003)
ice-2.2a	Ph	Sandfell	64.1100	-21.1990	14.0			0.7	Dixon (2003)
ice-2.2b	Ph	Sandfell	64.1100	-21.1990	11.0			2.5	Dixon (2003)
ice-10.2	Ph	Mælifell	64.1040	-21.2020	16.0			5.8	Dixon (2003)
ice-11.2	Ph	Sandfell	64.1100	-21.1990	17.0			6.9	Dixon (2003)
ice-16	Ph	Eldborg	63.8570	-22.0050	18.0			12.3	Dixon (2003)
ice-25	Ph	Bleikhóll	63.8630	-22.3560	16.0			11.2	Dixon (2003)
VEY/1	Ph	Valseyri	65.8500	-23.2500	32.7				Ellam & Stuart (2004)
SKI/NWP	Ph	Sauðanes/Skagafjall	65.9833	-23.7333	35.1				Ellam & Stuart (2004)
SDA1	Ph	Selárdalur	65.7500	-24.0333	37.0				Ellam & Stuart (2004)
ED1	Ph	Hestur	65.5000	-24.3000	30.0				Ellam & Stuart (2004)
VP/1	Ph	Vopnafjörður	65.7500	-14.8333	14.6				Ellam & Stuart (2004)
DICE5	Gl	SW of Mælifell	64.0964	-21.2019	12.7			88	Burnard & Harrison-(2005)
DICE7	Gl	Bæjarfjall	64.1061	-21.1711	13.1			234	Burnard & Harrison-(2005)

Continued

Sample	Phase	Location	Latitude	Longitude	R_m/R_A	X	R_c/R_A	[He] ^a	Reference
DICE8	Gl	Ölfusvatnsfjöll	64.1303	-21.1311	15.6			21	Burnard & Harrison-(2005)
DICE10	Gl	Dagmálafell	64.1769	-21.0503	17.8			1285	Burnard & Harrison-(2005)
DICE13	Gl	Kálfstindar	64.2311	-20.9311	17.1			2	Burnard & Harrison-(2005)
DICE15	Gl	Kálfstindar	64.2311	-20.9311	17.0			12	Burnard & Harrison-(2005)
DICE9	Gl	Arnafell	64.2158	-21.0728	20.2			7	Burnard & Harrison-(2005)
DICE43	Gl	Hrómundartindur	64.0842	-21.1892	17.7			120	Burnard & Harrison-(2005)
MAE	Gl	Mælifell	64.1061	-21.1833	13.4			113	Burnard & Harrison-(2005)
DICE11	Gl	Dagmálafell	64.1769	-21.0503	17.2			5630	Burnard & Harrison-(2005)
Th-29	Ph	Þeistareykir	65.8833	-16.8333	12.2			1.3	Macpherson et al. (2005)
NAL-611	Ph	Kistufell	64.8000	-17.2333	16.6			1	Macpherson et al. (2005)
NAL-688	Ph	Eggert	65.2500	-16.4833	8.0			1.2	Macpherson et al. (2005)
NAL-688	Ph	Eggert	65.2500	-16.4833	5.9			1.3	Macpherson et al. (2005)
NAL-239	Ph	Ketildyngja	65.4500	-16.7167	10.6			7	Macpherson et al. (2005)
NAL-625	Ph	Vaðalda	64.9333	-16.4667	34.3			0.4	Macpherson et al. (2005)
NAL-625	Ph	Vaðalda	64.9333	-16.4667	30.5			0.2	Macpherson et al. (2005)
NAL-625	Ph	Vaðalda	64.9333	-16.4667	20.2			0.4	Macpherson et al. (2005)
#9613	Ph	Ódádahraun	65.1500	-16.5333	7.6			1.2	Macpherson et al. (2005)
TRO-53	Ph	Trölladyngja	64.9000	-17.1000	8.3			0.3	Macpherson et al. (2005)
NAL-626	Ph	Fjallsendi	65.0500	-17.0833	17.3			17.4	Macpherson et al. (2005)
THJOR	Ph	Þjórsárdalur	64.1333	-20.1667	18.3			3.2	Macpherson et al. (2005)
Herðubreið	Gl	Herðubreið	65.1667	-16.3500	9.1			44.5	Macpherson et al. (2005)
NAL-496	Gl	Gæsahnjúkur	64.7667	-17.4833	17.6			2.5	Macpherson et al. (2005)
SAL-306	Gl	Bárðarbunga	64.7000	-17.5833	21.9			8.8	Macpherson et al. (2005)
NAL-688	Gl	Eggert	65.2500	-16.4833	8.9			127	Macpherson et al. (2005)
NAL-688	Gl	Eggert	65.2500	-16.4833	8.8			85	Macpherson et al. (2005)
NAL-355	Gl	Upptyppingar	65.0333	-16.2333	8.8			31	Macpherson et al. (2005)
NAL-356	Gl	Upptyppingar	65.0333	-16.2333	8.5			58.2	Macpherson et al. (2005)
NAL-355/6	Gl	Upptyppingar	65.0333	-16.2333	8.9			22.3	Macpherson et al. (2005)

Continued

Sample	Phase	Location	Latitude	Longitude	R_m/R_A	X	R_c/R_A	[He] ^a	Reference
KVK-169	Gl	Jarðfræðingaslóð	64.7667	-16.5000	8.5			8.9	Macpherson et al. (2005)
NAL-357	Gl	Upptýppingar	65.0333	-16.2333	5.0			0.6	Macpherson et al. (2005)
KVK-147	Gl	Hvannalindir	64.8667	-16.3500	2.6			0.8	Macpherson et al. (2005)
KVK-168	Gl	Jarðfræðingaslóð	64.7667	-16.6333	1.6			3.8	Macpherson et al. (2005)
SAL-575	Gl	Sólheimajökull	63.5333	-19.3833	14.6			1.5	Macpherson et al. (2005)
IC02-16-19084	Ph	Lambahraun	64.3843	-20.5549	13.6			0.34	Licciardi et al. (2006)
IC02-17-17338	Ph	Lambahraun	64.3836	-20.5564	13.4			0.2	Licciardi et al. (2006)
IC02-19-19323	Ph	Lambahraun	64.3644	-20.5531	12.7			0.59	Licciardi et al. (2006)
IC02-20-16373	Ph	Lambahraun	64.3629	-20.5514	13.7			0.11	Licciardi et al. (2006)
LEIT-1-1067	Ph	Leitahraun	63.9726	-21.4674	13.8			1.68	Licciardi et al. (2006)
LEIT-2-1374	Ph	Leitahraun	63.9738	-21.4671	13.9			0.7	Licciardi et al. (2006)
LEIT-3-1191	Ph	Leitahraun	63.9765	-21.4783	15.3			2.29	Licciardi et al. (2006)
LEIT-4-1131	Ph	Leitahraun	63.9822	-21.4773	14.2			0.6	Licciardi et al. (2006)
LEIT-5-1315	Ph	Leitahraun	63.9839	-21.4727	13.2			1.87	Licciardi et al. (2006)
LEIT-5-1129	Ph	Leitahraun	63.9838	-21.4727	15.8			0.88	Licciardi et al. (2006)
BUR-1-2410	Ph	Búrfellshraun	64.0592	-21.8744	14.0			0.41	Licciardi et al. (2006)
BUR-2-2401	Ph	Búrfellshraun	64.0892	-21.9679	12.9			0.56	Licciardi et al. (2006)
BUR-3-2713	Ph	Búrfellshraun	64.0896	-21.9690	12.5			2.66	Licciardi et al. (2006)
BUR-3-2780	Ph	Búrfellshraun	64.0896	-21.9690	11.4			0.08	Licciardi et al. (2006)
BUR-4-2585	Ph	Búrfellshraun	64.0917	-21.9704	13.5			0.21	Licciardi et al. (2006)
BUR-4-2854	Ph	Búrfellshraun	64.0917	-21.9704	14.7			1.35	Licciardi et al. (2006)
BUR-5-2732	Ph	Búrfellshraun	64.0935	-21.9685	13.1			0.26	Licciardi et al. (2006)
BUR-6-2792	Ph	Búrfellshraun	64.0871	-21.9689	13.5			0.56	Licciardi et al. (2006)
IC02-1-18787	Ph	Pingvallahraun	64.1645	-21.0369	14.5			1.69	Licciardi et al. (2006)
IC02-7-10543	Ph	Pingvallahraun	64.1649	-21.0368	11.0			0.43	Licciardi et al. (2006)
IC02-10-25131	Ph	Pingvallahraun	64.1562	-21.0480	15.1			0.87	Licciardi et al. (2006)
IC02-11-17430	Ph	Pingvallahraun	64.1561	-21.0480	14.5			0.27	Licciardi et al. (2006)
ICE 3	Gl	Stapafell	63.9106	-22.5224	13.9			1430	Brandon et al. (2007)

Continued

Sample	Phase	Location	Latitude	Longitude	R_m/R_A	X	R_c/R_A	[He] ^a	Reference
Ice 5	Gl	Dagmálafell	64.1747	-21.0485	17.2			2560	Brandon et al. (2007)
DMF 9101	Gl	Dagmálafell	64.1747	-21.0467	16.5			512	Brandon et al. (2007)
DMF 9101	Gl	Dagmálafell	64.1747	-21.0467	17.53			258	Brandon et al. (2007)
ICE 0	Ph	Hrúthálsar	65.3250	-16.5000	9.62			1.14	Brandon et al. (2007)
ICE 2	Ph	Lagafell	63.8851	-22.5367	11.18			3.9	Brandon et al. (2007)
ICE 2	Ph	Lagafell	63.8850	-22.5367	14.09			1.53	Brandon et al. (2007)
ICE 4a	Ph	Mælifell	64.1114	-21.1959	11.46			5.36	Brandon et al. (2007)
ICE 5	Ph	Dagmálafell	64.1747	-21.0485	16.62			12.2	Brandon et al. (2007)
DMF 9101	Ph	Dagmálafell	64.1747	-21.0467	16.4			11.7	Brandon et al. (2007)
ICE 8b	Ph	Skriðufell	64.1168	-19.9469	17.3			37.3	Brandon et al. (2007)
ICE 10	Ph	Hrúðurkarlarnir	64.5211	-20.8760	12.76			1.16	Brandon et al. (2007)
9805	Ph	Háleyjabunga	63.8197	-22.6525	10.89			0.52	Brandon et al. (2007)
9806	Ph	Vatnsheiði	63.8442	-22.3914	11.65			4.26	Brandon et al. (2007)
9809	Ph	Fagradalshraun	63.9117	-22.2947	12.74			1.92	Brandon et al. (2007)
9810	Ph	Eldborg	63.8558	-22.0020	19.0			13	Brandon et al. (2007)
9812	Ph	Ásar	63.9089	-21.3978	16.8			0.61	Brandon et al. (2007)
9815	Ph	Lyngfell	63.8586	-22.3120	15.83			3.48	Brandon et al. (2007)
IC02-60	Ph	Herðubreið	65.1782	-16.3614	12.4			0.52	Licciardi et al. (2007)
IC02-61	Ph	Herðubreið	65.1770	-16.3588	11.0			0.44	Licciardi et al. (2007)
IC02-62	Ph	Herðubreið	65.1773	-16.3587	10.8			0.51	Licciardi et al. (2007)
IC04-19	Ph	Herðubreið	65.1747	-16.3465	7.8			0.15	Licciardi et al. (2007)
IC04-20	Ph	Herðubreið	65.1838	-16.3391	8.7			0.2	Licciardi et al. (2007)
IC04-21	Ph	Herðubreið	65.1833	-16.3370	5.0			0.35	Licciardi et al. (2007)
IC03-29	Ph	Bláfjall	65.4434	-16.8587	10.1			4.52	Licciardi et al. (2007)
IC03-30	Ph	Bláfjall	65.4551	-16.8678	11.1			2.18	Licciardi et al. (2007)
IC03-31	Ph	Bláfjall	65.4568	-16.8661	9.9			1.63	Licciardi et al. (2007)
IC03-32	Ph	Bláfjall	65.4588	-16.8565	11.3			0.6	Licciardi et al. (2007)
IC03-25	Ph	Búrfell	65.5510	-16.6429	10.6			4.18	Licciardi et al. (2007)

Continued

Sample	Phase	Location	Latitude	Longitude	R_m/R_A	X	R_c/R_A	[He] ^a	Reference
IC03-26	Ph	Búrfell	65.5501	-16.6507	11.4			4.49	Licciardi et al. (2007)
IC03-27	Ph	Búrfell	65.5486	-16.6483	11.2			11.5	Licciardi et al. (2007)
IC03-28	Ph	Búrfell	65.5488	-16.6431	10.8			8.54	Licciardi et al. (2007)
IC02-52	Ph	Gæsafjöll	65.7838	-16.8822	10.5			5.61	Licciardi et al. (2007)
IC02-53	Ph	Gæsafjöll	65.7847	-16.8839	7.2			0.71	Licciardi et al. (2007)
IC02-54	Ph	Gæsafjöll	65.7856	-16.8709	12.7			1.12	Licciardi et al. (2007)
IC02-55	Ph	Gæsafjöll	65.7848	-16.8710	12.4			1.54	Licciardi et al. (2007)
IC02-56	Ph	Gæsafjöll	65.7868	-16.8926	11.4			0.12	Licciardi et al. (2007)
IC02-57	Ph	Gæsafjöll	65.7867	-16.9071	13.3			1.49	Licciardi et al. (2007)
IC03-22	Ph	Hafrafell	66.0500	-16.3452	21.0			3.84	Licciardi et al. (2007)
IC03-23	Ph	Hafrafell	66.0503	-16.3464	21.4			2.32	Licciardi et al. (2007)
IC03-19	Ph	Sandfell	66.1145	-16.3271	21.6			2.85	Licciardi et al. (2007)
IC03-20	Ph	Sandfell	66.1161	-16.3353	20.2			2.3	Licciardi et al. (2007)
IC03-21	Ph	Sandfell	66.1171	-16.3466	21.0			1.24	Licciardi et al. (2007)
IC02-58	Ph	Snarstaðarnúpur	66.3525	-16.4723	22.7			0.84	Licciardi et al. (2007)
IC02-63	Ph	Hlöðufell	64.4171	-20.5379	8.9			0.75	Licciardi et al. (2007)
IC02-64	Ph	Hlöðufell	64.4180	-20.5340	13.4			0.07	Licciardi et al. (2007)
IC02-65	Ph	Hlöðufell	64.4180	-20.5380	12.9			1.83	Licciardi et al. (2007)
IC04-6	Ph	Högnhöfði	64.3583	-20.4996	17.0			2.94	Licciardi et al. (2007)
IC04-8	Ph	Högnhöfði	64.3574	-20.4998	16.9			0.73	Licciardi et al. (2007)
IC04-11	Ph	Skriða	64.3557	-20.6842	14.0			0.41	Licciardi et al. (2007)
IC04-12	Ph	Skriða	64.3537	-20.6819	13.7			0.98	Licciardi et al. (2007)
IC03-14	Ph	Rauðafell	64.3234	-20.5818	2.5			5.59	Licciardi et al. (2007)
IC03-15	Ph	Rauðafell	64.3248	-20.5785	12.4			0.38	Licciardi et al. (2007)
IC03-16	Ph	Rauðafell	64.3248	-20.5782	10.8			0.68	Licciardi et al. (2007)
IC03-11	Ph	Hvalfell	64.3848	-21.1945	16.1			0.23	Licciardi et al. (2007)
IC03-12	Ph	Hvalfell	64.3876	-21.2010	13.7			0.09	Licciardi et al. (2007)
IC03-13	Ph	Hvalfell	64.3886	-21.2055	12.0			0.66	Licciardi et al. (2007)

Continued

Sample	Phase	Location	Latitude	Longitude	R_m/R_A	X	R_c/R_A	[He] ^a	Reference
IC03-6	Ph	Geitafell	63.9410	-21.5226	16.7			1.62	Licciardi et al. (2007)
IC03-7	Ph	Geitafell	63.9421	-21.5216	17.3			1.03	Licciardi et al. (2007)
IC03-8	Ph	Geitafell	63.9405	-21.5235	16.5			1.2	Licciardi et al. (2007)
HAIN	Ph	Heimaey	63.4000	-20.3000	11.05			2.95	Debaille et al. (2009)
SAL690	Ph	Katla	63.6700	-18.8300	16.78			10.7	Debaille et al. (2009)
SAL690B	Ph	Katla	63.6700	-18.8300	18.06			4.75	Debaille et al. (2009)
SAL768	Ph	Öræfajökull	63.9000	-16.6000	7.69			13.6	Debaille et al. (2009)
NAL759	Ph	Snæfell	64.8000	-15.5700	7.06			8.58	Debaille et al. (2009)
ICE-3	Gf	Nesjavellir	64.0960	-21.2800	14.75	839	14.77		Füri et al. (2010)
ICE08-11	Gf	Nesjavellir	64.0935	-21.4412	13.97	84.5	14.13		Füri et al. (2010)
ICE08-12	Gf	Nesjavellir	64.0935	-21.4412	13.48	59	13.69		Füri et al. (2010)
ICE-5	Gf	Svartsengi	63.8758	-22.4352	14.67	383	14.7		Füri et al. (2010)
ICE-6	Gf	Svartsengi	63.8758	-22.4352	14.24	214	14.3		Füri et al. (2010)
PBICE-1	Gf	Reykjanes	63.8185	-22.6846	8.99	10.1	9.69		Füri et al. (2010)
PBICE-2	Gf	Reykjanes	63.8185	-22.6846	11.91	137	11.97		Füri et al. (2010)
PBICE-3	Gf	Krísuvík	63.8953	-22.0553	13.87	194	13.92		Füri et al. (2010)
PBICE-4	Gf	Krísuvík	63.8953	-22.0553	2.62	2.3	3.5		Füri et al. (2010)
ICE08-14	Gf	Krísuvík	63.8953	-22.0554	13.83	63.3	14.03		Füri et al. (2010)
ICE08-15	Gf	Krísuvík	63.8953	-22.0554	13.89	205	13.95		Füri et al. (2010)
PBICE-9	Gf	Hengill	64.0200	-21.3949	12.27	14.7	12.39		Füri et al. (2010)
PBICE-12	Gf	Hengill	64.0200	-21.3949	12.67	19.3	13.18		Füri et al. (2010)
ICE08-22	Gf	Hengill	64.0069	-21.3418	15.69	84.7	15.86		Füri et al. (2010)
PBICE-13	Gf	Little Geysir	64.3107	-20.3024	16.59	72.8	16.77		Füri et al. (2010)
PBICE-14	Gf	Little Geysir	64.3107	-20.3024	15.99	70	16.17		Füri et al. (2010)
PBICE-10	Gf	Kerlingarfjöll	64.6436	-19.2881	14.22	28.7	14.61		Füri et al. (2010)
PBICE-11	Gf	Hveravellir	64.8654	-19.5583	13.68	32.1	14.01		Füri et al. (2010)
PBICE-16	Gf	Hveragerði	64.0223	-21.1940	16.89	51.1	17.15		Füri et al. (2010)
PBICE-8	Gf	Hveragerði	64.0223	-21.1940	17.08	40.7	17.41		Füri et al. (2010)

Continued

Sample	Phase	Location	Latitude	Longitude	R_m/R_A		R_c/R_A	[He] ^a	Reference
PBICE-5	Gf	Landmannalaugar	63.9812	-19.0893	1.26	2.5	1.39		Füri et al. (2010)
ICE08-26	Gf	Landmannalaugar	63.9924	-19.1005	1.24	3.4	1.35	17.5	Füri et al. (2010)
ICE08-29	Gf	Landmannalaugar	63.9892	-19.1117	3.28	4.6	3.92		Füri et al. (2010)
ICE08-30	Gf	Landmannalaugar	63.9908	-19.0629	4.28	3.4	5.64	680.1	Füri et al. (2010)
ICE08-17	Gf	Köldukvíslarbotnar	64.5709	-18.1111	3.04	3	4.05	6.3	Füri et al. (2010)
ICE08-18	Gf	Köldukvíslarbotnar	64.5709	-18.1111	2.19	4.7	2.51	10.9	Füri et al. (2010)
ICE08-16	Gf	Vonarskarð	64.6923	-17.8965	17.27	33.4	17.77		Füri et al. (2010)
ICE08-21	Gf	Vonarskarð	64.6923	-17.8965	18.86	50.5	19.22		Füri et al. (2010)
ICE08-13	Gf	Vonarskarð	64.6908	-17.8816	15.41	11.8	16.74	191.9	Füri et al. (2010)
ICE-11	Gf	Krafla	65.7045	-16.7451	8.86	72.1	8.97		Füri et al. (2010)
ICE-12	Gf	Krafla	65.7045	-16.7451	8.75	121	8.81		Füri et al. (2010)
ICE-10	Gf	Krafla	65.7087	-16.7608	5.58	7.94	6.24		Füri et al. (2010)
ICE-17	Gf	Krafla	65.7087	-16.7608	8.84	158	8.89		Füri et al. (2010)
PBICE-20	Gf	Krafla	65.7217	-16.7876	8.36	144	8.4		Füri et al. (2010)
ICE08-06	Gf	Krafla	65.7217	-16.7876	8.89	314	8.91		Füri et al. (2010)
ICE08-10	Gf	Krafla	65.7194	-16.7882	10.36	2361	10.36		Füri et al. (2010)
PBICE-15	Gf	Námafjall	65.6418	-16.8099	3.1	4	3.63		Füri et al. (2010)
ICE08-03	Gf	Námafjall	65.6408	-16.8096	9.27	28	9.58		Füri et al. (2010)
ICE08-02	Gf	Námafjall	65.6408	-16.8084	10.26	558	10.28		Füri et al. (2010)
PBICE-7	Gf	Þeistareykir	65.8759	-16.9567	8.58	23	8.86		Füri et al. (2010)
ICE08-09	Gf	Þeistareykir	65.8731	-16.9702	10.1	242	10.13		Füri et al. (2010)
PBICE-18	Gf	Askja, Víti crater	65.0446	-16.7254	9.08	130	9.13		Füri et al. (2010)
ICE08-05	Gf	Askja, Víti crater	65.0467	-16.7248	9.7	550	9.71		Füri et al. (2010)
ICE08-19	Gf	Kverkfjöll	64.6750	-16.6927	8.37	131	8.43		Füri et al. (2010)
ICE08-20	Gf	Kverkfjöll	64.6750	-16.6927	9.06	103	9.14		Füri et al. (2010)
ICE-8	Gf	Seljavellir	63.5656	-19.6086	18.46	69.9	18.72	6232.5	Füri et al. (2010)
ICE-9	Gf	Seljavellir	63.5656	-19.6086	19.02	107	19.19	4502.9	Füri et al. (2010)
ICE-18	Gf	Lýsuhóll	64.8446	-23.2196	9.09	646	9.11		Füri et al. (2010)

Continued

Sample	Phase	Location	Latitude	Longitude	R_m/R_A	X	R_c/R_A	[He] ^a	Reference
ICE-7	Gf	Lýsuhóll	64.8446	-23.2196	9.34	672	9.34		Füri et al. (2010)
ICE-22	Gf	Hæðarendi	64.0755	-20.8601	18.62	283	18.69		Füri et al. (2010)
PBICE-17	Gf	Selfoss	63.9462	-20.9606	16.92	8.8	18.55		Füri et al. (2010)
PBICE-19	Gf	Selfoss	63.9462	-20.9606	17.79	62	18.01		Füri et al. (2010)
ICE08-27	Gf	Þjórárdalslaug	64.1616	-19.8115	21.67	114	21.86		Füri et al. (2010)
ICE08-28	Gf	Þjórárdalslaug	64.1616	-19.8115	21.74	110	21.93		Füri et al. (2010)
ICE08-23	Gf	Flúðir	64.1293	-20.3236	17.21	36.7	17.67	793.5	Füri et al. (2010)
ICE08-25	Gf	Ormsstaðir	64.0416	-20.6629	21.27	39.6	21.8	3262.4	Füri et al. (2010)
ICE08-24	Gf	Eyvík	64.0468	-20.6998	22.04	119	22.22	8645.6	Füri et al. (2010)
ICE-23	Gf	Hveravík	65.6984	-21.5598	24.09	74.2	24.4	1316.4	Füri et al. (2010)
ICE-24	Gf	Hveravík	65.6984	-21.5598	24.02	59.7	24.41	1544.9	Füri et al. (2010)
ICE-25	Gf	Laugarhóll	65.7810	-21.5203	8.43	5.16	10.22		Füri et al. (2010)
ICE-26	Gf	Laugarhóll	65.7810	-21.5203	8.73	4.32	11.06		Füri et al. (2010)
ICE-28	Gf	Goðdalur	65.8277	-21.5917	15.48	6.01	18.37	179.1	Füri et al. (2010)
ICE-29	Gf	Gjögur	66.0005	-21.3201	15.83	38.5	16.22		Füri et al. (2010)
ICE-30	Gf	Gjögur	66.0005	-21.3201	15.61	18.6	16.44	457	Füri et al. (2010)
ICE-31	Gf	Krossnes	66.0505	-21.5063	26.76	42.4	27.38		Füri et al. (2010)
ICE-33	Gf	Krossnes	66.0505	-21.5063	26.38	48.7	26.91		Füri et al. (2010)
ICE-34	Gf	Laugaland	66.0199	-22.3955	3.39	11.4	3.62		Füri et al. (2010)
ICE-36	Gf	Heyárdalur	65.8397	-22.6778	16.32	11.7	17.75	323.7	Füri et al. (2010)
ICE-37	Gf	Laugar	66.1113	-23.4548	11.11	5.63	13.3	8659.3	Füri et al. (2010)
ICE-38	Gf	Laugardalsá	65.6564	-23.9102	23.59	31.2	24.34	1389.3	Füri et al. (2010)
ICE-39	Gf	Reykhólar	65.4544	-22.1980	12.93	12.2	13.99	172.9	Füri et al. (2010)
SKARD-1	Gl	Skarðsmýrarfjall	64.0438	-21.3583	12.94			9.27	Füri et al. (2010)
VIF-1	Gl	Vífilsfell	64.0487	-21.5402	12.97			45.18	Füri et al. (2010)
MID-1	Gl	Miðfell	64.1747	-21.0475	16.65			3177	Füri et al. (2010)
MID-1	Gl	Miðfell	64.1747	-21.0475	17.22			3447	Füri et al. (2010)
MID-2	Gl	Arnarfell	64.2173	-21.0700	15.58			35.35	Füri et al. (2010)

Continued

Sample	Phase	Location	Latitude	Longitude	R_m/R_A	X	R_c/R_A	[He] ^a	Reference
MID-3	GI	Kálfstindar	64.2184	-20.8858	14.06			868.19	Füri et al. (2010)
NES-1	GI	Nesjavellir	64.1003	-21.2473	15.75			139.64	Füri et al. (2010)
OLF-1	GI	Ölfusvatnsfjöll	64.1158	-21.1407	14.49			258.17	Füri et al. (2010)
THREN-1	GI	Þrengsli	64.0013	-21.4626	13.62			48.8	Füri et al. (2010)
REY-1	GI	Reykjanes viti	63.8124	-22.7137	14.2			623.43	Füri et al. (2010)
HRA-1	GI	Hraunsvík	63.8519	-22.3687	14.16			27.06	Füri et al. (2010)
MAE-1	GI	Mælifell	64.1071	-21.1819	12.48			400.04	Füri et al. (2010)
LON-1	GI	Lönguhlíðar	63.9717	-21.9451	15.49			24.74	Füri et al. (2010)
KLE-1	GI	Kleifarvatn	63.9112	-22.0121	12.64			3.19	Füri et al. (2010)
HEL-2	GI	Helgafell	64.0161	-21.8424	12.37			7.91	Füri et al. (2010)
ICE08R-07	GI	Stakur	63.9964	-21.8887	11.43			15.53	Füri et al. (2010)
A1	GI	Ármannsfell	64.3204	-20.9955	15.26			168.51	Füri et al. (2010)
A2	GI	Þórólfsfell	64.4488	-20.5173	14.01			154.03	Füri et al. (2010)
A3	GI	Hlöðufell	64.4290	-20.5704	15.18			29.23	Füri et al. (2010)
A4	GI	Fagradalsfjöll	64.4528	-20.3061	15.36			24.23	Füri et al. (2010)
A6	GI	Bláfell	64.5156	-19.8878	15.36			50.36	Füri et al. (2010)
A8	GI	Þverbrekknamúli	64.7232	-19.6146	14.52			22.08	Füri et al. (2010)
A9	GI	Arnarbæli	65.0141	-19.5891	21.05			831.47	Füri et al. (2010)
STAK-1	GI	Stakksá	64.2949	-20.3648	14.73			4.93	Füri et al. (2010)
KVIH-1	GI	Kvíhólafljöll	65.8402	-16.9862	9.39			13.04	Füri et al. (2010)
NAL-837	GI	Kvíhólafljöll	65.8402	-16.9862	9.41			26.08	Füri et al. (2010)
NAL-213	GI	Hvammsfjöll	65.3638	-16.6741	12.49			85.51	Füri et al. (2010)
NAL-216	GI	Hvammsfjöll	65.3608	-16.6865	12.84			578.61	Füri et al. (2010)
NAL-263	GI	V-Skógamannafjöll	65.5822	-16.5648	9.25			2826.9	Füri et al. (2010)
NAL-265	GI	V-Skógamannafjöll	65.5883	-16.5655	9.01			91.63	Füri et al. (2010)
NAL-281	GI	Herðubreiðarfjöll	65.3696	-16.3749	10.36			1255	Füri et al. (2010)
NAL-440	GI	Hrímalda	64.9248	-17.0856	8.84			4.68	Füri et al. (2010)
NAL-455	GI	Kverkfjöll	64.7384	-16.6223	2.27			5.04	Füri et al. (2010)

Continued

Sample	Phase	Location	Latitude	Longitude	R_m/R_A	X	R_c/R_A	[He] ^a	Reference
NAL-458	GI	Búrfell	65.5678	-16.6430	3.04			5.07	Füri et al. (2010)
NAL-460	GI	Þeistareykir/Kistufjall	65.8792	-17.1556	4.91			2.96	Füri et al. (2010)
NAL-461	GI	Þeistareykir/Lambafjall	65.8385	-17.1126	4.27			2.74	Füri et al. (2010)
NAL-500	GI	Gæsavatn	64.7806	-17.5113	17.57			205.34	Füri et al. (2010)
NAL-537	GI	Herðubreiðarfjöll	65.3583	-16.4009	11.4			277.95	Füri et al. (2010)
NAL-541	GI	Herðubreiðarfjöll	65.3651	-16.4437	10.71			15.85	Füri et al. (2010)
NAL-543	GI	Herðubreiðarfjöll	65.3492	-16.4318	9.44			234.01	Füri et al. (2010)
NAL-584	GI	Dyngjufjöll Ytri	65.1617	-16.9243	19.69			53.1	Füri et al. (2010)
NAL-585	GI	Upptýppingar	65.0280	-16.2290	8.66			58.58	Füri et al. (2010)
NAL-595	GI	Kistufell	64.7899	-17.1823	15.69			916.96	Füri et al. (2010)
NAL-600	GI	Urðarháls	64.8394	-17.1515	13.78			336.62	Füri et al. (2010)
NAL-611	GI	Kistufell	64.7984	-17.2003	16.94			1323.7	Füri et al. (2010)
NAL-828	GI	Hrúthálsar	65.3238	-16.5028	8.82			545.68	Füri et al. (2010)
HS92-15	GI	Bláfjall	65.4266	-16.8156	10.75			1636.7	Füri et al. (2010)
HS92-16	GI	Bláfjall	65.4251	-16.8161	11.83			31.4	Füri et al. (2010)
KVK 77	GI	Kverkfjöll	64.8167	-16.4833	8.05			46.37	Füri et al. (2010)
A11	GI	Hnottóttalda	64.5220	-18.4717	24.26			136.41	Füri et al. (2010)
A12/ICE08R-08	GI	N- og S-Hágöngur	64.5697	-18.1997	18.06			31.77	Füri et al. (2010)
A13/ICE08R-09	GI	Skerðingar	64.5716	-18.0706	20.86			52.48	Füri et al. (2010)
A15	GI	Vatnsfellsvirkjun	64.2018	-19.3883	7			2.91	Füri et al. (2010)
A16/ICE08R-10	GI	Bláfjall	64.3717	-18.2484	18.09			56.71	Füri et al. (2010)
A18/ICE08R-12	GI	Outcrop close to Dór	64.3813	-18.2506	19.79			302.16	Füri et al. (2010)
ICE08R-13	GI	Bláfjall	64.3896	-18.2292	19.39			517.69	Füri et al. (2010)
A19/ICE08R-14	GI	Ljósufjöll	64.2433	-18.5827	22.65			27.32	Füri et al. (2010)
A20/ICE08R-15	GI	Kambsfell	64.8274	-17.7555	20.33			597.3	Füri et al. (2010)
A21/ICE08R-16	GI	Gnjótsá near Kambsfell	64.8269	-17.7023	22.16			1099.82	Füri et al. (2010)
A22/ICE08R-17	GI	North of Valafell	64.7305	-17.7085	20.15			1033.66	Füri et al. (2010)
A23/ICE08R-18	GI	Gully near Valafell	64.7237	-17.7222	21.02			298.54	Füri et al. (2010)

Continued

Sample	Phase	Location	Latitude	Longitude	R_m/R_A	X	R_c/R_A	[He] ^a	Reference
A24	Gl	Mið-Bálkafell	64.6730	-17.7661	25.91			56.2	Füri et al. (2010)
A25/ICE08R-19	Gl	Svarthöfði	64.6425	-17.8686	21.86			15.62	Füri et al. (2010)
A26	Gl	Vonarskarð	64.6923	-17.8965	19.89			186.36	Füri et al. (2010)
A27	Gl	Kirkjufellsvatn	63.9790	-18.8963	19.67			115.5	Füri et al. (2010)
A28	Gl	Klappagil	63.9741	-18.7922	1.87			4.09	Füri et al. (2010)
A29	Gl	Hörðufell	63.9690	-18.6798	8.76			1.09	Füri et al. (2010)
A30	Gl	Hellnaá	64.0614	-18.5340	18.59			5.72	Füri et al. (2010)
A31	Gl	Hrútabjörg	64.1103	-18.4616	12.17			3.09	Füri et al. (2010)
A32	Gl	NW of Grænifjallgarður	64.1058	-18.5154	18.07			132.44	Füri et al. (2010)
A33	Gl	Breiðbak	64.1059	-18.5687	18.99			3.79	Füri et al. (2010)
A34	Gl	Hnausar	64.0878	-19.0542	10.55			2.3	Füri et al. (2010)
A35	Gl	Sigalda	64.1722	-19.1385	20.59			193.15	Füri et al. (2010)
A36/ICE08R-23	Gl	Heljargjá	64.3222	-18.4605	19.65			6.05	Füri et al. (2010)
A37/ICE08R-24	Gl	Miklagljúfur	64.3205	-18.4326	19.23			8.31	Füri et al. (2010)
A38/ICE08R-25	Gl	Fellsendavatn	64.1885	-18.9570	2.19			2.55	Füri et al. (2010)
ICE08R-20	Gl	Fontur, craters	64.2518	-18.6523	1.16			2.41	Füri et al. (2010)
RET-1/VES-1	Gl	Réttarfell (Þórsmörk)	63.6721	-19.4923	18.93			90.56	Füri et al. (2010)
MID-1	Ph	Miðfell	64.1747	-21.0475	16.23			10.44	Füri et al. (2010)
MID-1	Ph	Miðfell	64.1747	-21.0475	17.28			11.11	Füri et al. (2010)
BUR-1	Ph	Búrfell	63.8999	-21.4622	13.05			2.69	Füri et al. (2010)
THREN-1	Ph	Þrengsli	64.0013	-21.4626	12.59			5.04	Füri et al. (2010)
D-2	Ph	Háleyjarbunga	63.8154	-22.6453	14.34			7.71	Füri et al. (2010)
GRIN-1	Ph	Grindavík	63.8460	-22.4139	10.27			0.57	Füri et al. (2010)
VATN-1	Ph	Vatnsheiði	63.8593	-22.3718	11.92			3.28	Füri et al. (2010)
ISO-1	Ph	Ísólfskáli	63.8608	-22.3178	16.3			6.09	Füri et al. (2010)
MAE-1	Ph	Mælifell	64.1071	-21.1819	12.94			14.37	Füri et al. (2010)
MAE-1	Ph	Mælifell	64.1071	-21.1819	12.44			12.37	Füri et al. (2010)
Th-29	Ph	Þeistareykir	65.9310	-17.0726	6.11			0.14	Füri et al. (2010)

Continued

Sample	Phase	Location	Latitude	Longitude	R _m /R _A	X	R _c /R _A	[He] ^a	Reference
BORG-1	Ph	Borgarhraun	65.8425	-16.9925	7.91			1.97	Füri et al. (2010)
ICE08R-01	Ph	Bjarnardalsá	64.8339	-21.4891	20.34			2.02	Füri et al. (2010)
ICE08R-01	Ph	Bjarnardalsá	64.8339	-21.4891	14.78			1.91	Füri et al. (2010)
ICE08R-02	Ph	Selárdalur	65.7621	-24.0431	34.92			1.5	Füri et al. (2010)
ICE08R-02	Ph	Selárdalur	65.7621	-24.0431	36.76			3.55	Füri et al. (2010)
ICE08R-03	Ph	Vatnseyri	65.8514	-23.2534	26.08			0.4	Füri et al. (2010)
ICE08R-04b	Ph	Ekkisdalur	65.9568	-23.3186	36.38			1.08	Füri et al. (2010)
ICE08R-04b	Ph	Ekkisdalur	65.9568	-23.3186	2.7			0.67	Füri et al. (2010)
Lambadalur	Ph	Dýrafjörður	65.8500	-23.2667	21.64			0.2	Füri et al. (2010)
Lambadalur	Ph	Dýrafjörður	65.8500	-23.2667	21.39			0.61	Füri et al. (2010)
408738	Ph	Snæfell	64.8050	-15.5990	6.93			7.99	Peate et al. (2010)
408739	Ph	Snæfell	64.8070	-15.5900	7.12			4.11	Peate et al. (2010)
408740	Ph	Snæfell	64.7960	-15.5990	7.14			1.19	Peate et al. (2010)
408744	Ph	Snæfell	64.7990	-15.6100	7.2			7.8	Peate et al. (2010)
408754	Ph	Snæfell	64.8170	-15.6970	7.02			2.93	Peate et al. (2010)
408755	Ph	Snæfell	64.8530	-15.5790	6.95			7.13	Peate et al. (2010)
408757	Ph	Snæfell	64.8500	-15.5370	7.51			16.3	Peate et al. (2010)
408764	Ph	Gullborgarhraun	64.8930	-22.3320	8.52			13.3	Peate et al. (2010)
408765	Ph	Búðahraun	64.8190	-23.3870	6.25			1.95	Peate et al. (2010)
408767	Ph	Hreggnasi	64.8500	-23.8330	7.93			3.34	Peate et al. (2010)
408770	Ph	Bersekjahraun	64.9480	-22.9850	8.54			8.42	Peate et al. (2010)
408771	Ph	Svelgsárhraun	64.9760	-22.6750	8.64			13.8	Peate et al. (2010)
408775	Ph	Hvammsmúli	63.5740	-19.8700	17.13			0.1	Peate et al. (2010)
408783	Ph	Heimaey/Stórhöfði	63.4040	-20.2750	14.51			11.2	Peate et al. (2010)
408784	Ph	Heimaey/Stórhöfði	63.4040	-20.2770	13.11			4.26	Peate et al. (2010)
408785	Ph	Heimaey/Há	63.4420	-20.2830	13.7			2.08	Peate et al. (2010)
STAP-1	Gl	Stapafell	63.9081	-22.5250	14.15	70485	14.15	48.4	Halldórsson et al. (2016)
FROST-1	Gl	Frostastaðavatn	64.0106	-19.0769	1.1	2.7	1.16	10.3	Halldórsson et al. (2016)

Continued

Sample	Phase	Location	Latitude	Longitude	R _m /R _A	X	R _c /R _A	[He] ^a	Reference
TRI-1	Gl	Þríhyrningur	63.8000	-19.9519	25.2	309	25.28	473	Halldórsson et al. (2016)
TRI-2	Gl	Þríhyrningur	63.7928	-19.9247	25.66	1125	25.68	123	Halldórsson et al. (2016)
TRI-3	Gl	Þríhyrningur	63.7925	-19.9243	24.94	100	25.18	203	Halldórsson et al. (2016)
ENG-1	Gl	Engifjall	63.7839	-20.0265	22.29	271	22.37	271	Halldórsson et al. (2016)
THOR-1	Gl	Þórólfsfell	63.7080	-19.7086	2.79	2.9	3.72	0.37	Halldórsson et al. (2016)
THOR-2	Gl	Þórólfsfell	63.7042	-19.6409	2.62	3.5	3.27	0.94	Halldórsson et al. (2016)
STORID-1	Gl	Stóri-Dímon	63.6781	-19.9476	8.17	26	8.45	1.69	Halldórsson et al. (2016)
SELJA-1	Gl	Seljalandsfoss	63.6255	-19.9873	8.18	3.8	10.74	14.1	Halldórsson et al. (2016)
BHE-43	Gl	Ófærugil	64.0534	-19.7311	20.58	264	20.66	307	Halldórsson et al. (2016)
BHE-44	Gl	Ytri-Rangá	64.0555	-19.7751	20.79	87	21.02	274	Halldórsson et al. (2016)
SAL601	Gl	Katla	63.5011	-18.9881	17.79	16	18.92	4.12	Halldórsson et al. (2016)
OLAF-1	Gl	Ólafsvíkurenni	64.8942	-23.7967	2.36	3	3.03	0.81	Halldórsson et al. (2016)
HNAUS-1	Gl	Hnausagil	64.8158	-23.6311	4.79	1.9	9.03	2.41	Halldórsson et al. (2016)
BOTN-1	Gl	Botnsfjall	64.7961	-23.6469	3.88	2.2	6.3	0.96	Halldórsson et al. (2016)

^a: [He] is reported in ncm³STP/g for all glass and phenocryst samples. For geothermal samples [He] is reported in ncm³STP/gH₂O in most cases, exceptions are Poreda et al. (1992) and Sano et al. (1985) report [He] in ppm and Marty et al. (1991) report [He] in μmole/kg.